7-2022

Targeting Mutated KRAS and Galectin-1 in Pancreatic Cancer

Ana Izavelle Martinez Bulnes
The University of Texas Rio Grande Valley

TARGETING MUTATED KRAS AND GALECTIN-1 IN PANCREATIC CANCER

A Thesis

by

ANA IZAVELLE MARTINEZ BULNES

Submitted in Partial Fulfillment of the

Requirements for the Degree of

MASTER OF SCIENCE

Major Subject: Biochemistry and Molecular Biology

The University of Texas Rio Grande Valley

July 2022

TARGETING MUTATED KRAS AND GALECTIN-1 IN PANCREATIC CANCER

A Thesis

by

ANA IZAVELLE MARTINEZ BULNES

COMMITTEE MEMBERS

Dr. Sheema Khan

Chair of Committee

Dr. Subhash Chauhan

Committee Member

Dr. Murali Yallapu

Committee Member

Dr. Robert Dearth

Committee Member

July 2022

ABSTRACT

Martinez Bulnes, Ana I., Targeting Mutated-KRAS and Galectin-1 in Pancreatic Cancer. Master of Science (MS), July, 2022, 85 pp., 1 table, 27 figures, references, 93 titles.

The poor patient survival rate in pancreatic ductal adenocarcinoma (PDAC) remains a challenge. KRAS activating point mutation on codon-12 is found in 70–95 percent of PDAC patients, and no progress in inhibiting KRAS has been obtained thus far. $KRAS^{G12D}$ is a transcription factor that controls cell proliferation, differentiation, and apoptosis. Recent preliminary and published research indicates that Galectin-1 (Gal-1) levels are high in both PDAC and stromal cells, which modulates tumor microenvironment and metastasis. As a result, we created a new combination treatment for PDAC that targets both proliferation and metastasis in PDAC by targeting mutant $KRAS^{G12D}$ and Gal-1. This includes the delivery of $KRAS^{G12D}$ inhibiting siRNA ($siKRAS^{G12D}$) using a superparamagnetic iron oxide nanoparticle (SPION) and a Gal-1 inh.

A patented SPION nano-formulation was used to deliver $siKRAS^{G12D}$ and investigated in conjunction with Gal-1 inh for its anticancer efficacy. Particles were investigated for size, physico-chemical characterization (Dynamic light scattering), hemocompatibility (hemolysis assay) and the complexation of siKRAS (gel retardation assay). Cellular internalization and uptake of the particles were investigated. Anti-cancer efficacy was

determined using in vitro functional assays for cell viability (MTT), migration (Boyden chambers), invasion (Matrigel), clonogenicity, wound healing, tumor spheroid formation, and in a mouse model.

Our findings show that the SPION-siKRAS formulation has an excellent particle size/zeta potential. SPION-siKRAS internalized effectively in PDAC cells, suppressing KRASG12D as well as its downstream targets, YAP and PDL-1. Cell growth was decreased when siKRAS and Gal-1 were both targeted. It decreased PDAC cell growth, clonogenicity, migration, and invasion. This resulted in the activation of death-related pathways in KRASG12D cells, such as Bax, bcl-2, and PARP cleavage. Surprisingly, the formulation was particularly efficient in reducing KRASG12D and tumor spheroid formation in 3D cell models, resembling the heterogeneity and pathogenesis of PDAC. This adds to the clinical confirmation of SPION-siKRAS particles' ability to effectively suppress KRAS expression. SPION-siKRAS also demonstrated hemocompatibility and stability, suggesting that it has the potential to silence KRAS without being hazardous to the body. In KPC mouse model C57BL/6J mice, the formulation effectively silenced $KRAS^{G12D}$ and reduced tumor development and metastasis.

This gene therapy targeting $KRAS^{G12D}$ mutation with Gal-1 inhibition has the ability to modify the oncogenic network and tumor microenvironment, resulting the repression of growth, metastasis, chemoresistance, and improvement in patient survival. This project will create a fresh, long-term treatment strategy to target PDAC development and patient survival.

DEDICATION

This achievement, Master of Science, would not have been possible without the unending love and support of my mother (Ana J. Bulnes Larios), father (Juan R. Martinez Midence), brother (Juan R. Martinez Bulnes), and fiancé (Jakob C. Rassman), who have been nothing but supportive throughout it all. I would like to thank my grandparents, aunts, uncles, and cousins for your constant words of encouragement and support. I would also like to thank the most amazing, supportive, and encouraging lab mates I encountered. I dedicate my master's degree and everything it entails to my parents, the ones who gave me everything, the ones who made sure nothing essential was lacking in my life, thank you, I love you, I thank you for helping to mold the woman that I am today.

ACKNOWLEDGMENTS

I shall be eternally thankful to Dr. Sheema Khan, my thesis supervisor, for all her guidance and advise. She motivated me to complete this project with her immense patience and guidance, from research design to data processing to, manuscript editing. She exposed me to amazing opportunities within the research field that allowed me to grow as person and as a researcher. My gratitude goes to the members of my dissertation committee: Dr. Murali Yallapu, Dr. Subhash C Chauhan, Dr. Robert Dearth and Dr. Sheema Khan. Their counsel, feedback, and constructive criticisms on my thesis helped to assure the intellectual quality of my work. I would also like to thank my colleagues in the Department of Immunology and Microbiology, Swathi Hola, Melida Flores Cantu, Orlando Garcia, Nycol Cotto, Samantha Lopez, Anyssa Rodriguez, Sophia Leslie, Swathi Hola, Melida Flores Cantu, Carlos Perez, Emmanuel Anning, Godwin Peasah-Darkwah, Dr. Neeraj Chauhan, Dr. Diego V.P., Partha Laskar, Dr. Fnu Shabnam, Dr. Mohammed Sikander; Dr. Sudhir Kotnala, and a special shoutout to my partner Poornima Shaji. Dr. Michael Persans, thank you from the bottom of my heart for believing in me even when I didn't. His guidance, suggestions, timely recommendations, excitement, and energy helped me earn a master's degree from the University of Texas Rio Grande Valley. My most grateful gratitude goes to my support system, my rocks, my team, thank you Mother, Father, Brother, and Fiancé, you all made this possible, I am eternally grateful. The work was supported by UTRGV Grant support (35000459) to Dr. Sheema Khan.

TABLE OF CONTENTS

Page

LIST OF TABLES

Page

LIST OF FIGURES

Page

CHAPTER I

INTRODUCTION

1. Statement of the problem

Pancreatic cancer (PanCa) is presently the third leading cause of death in the United States, and it is projected to be the second most in the next decade and the seventh leading cause worldwide. This year, an estimated 62,210 new cases have been reported, with 49,830 deaths. The aggressiveness of pancreatic tumor makes it difficult to cure and contributes to various levels of treatment resistant therapies. The poor prognosis is mostly the result of late diagnosis, significant genetic heterogeneity, ineffective therapy, and restricted surgical methods. However, the majority of patients are detected at an advanced stage, with metastases already present, and as a result, less than 20% of patients benefit from tumor excision. Chemotherapy may offer some advantages, but most attempts to modify current regimens fail in advanced clinical studies.

Pancreatic ductal adenocarcinoma (PDAC), accounts for 90% of PanCa occurrences. PDAC is the most frequent tumor in the pancreas, and it is one of the deadliest malignancies, with a 5-year survival rate of 10% (Hirt *et al*. 2022). PDAC is a highly invasive tumor with early metastatic potential for which therapeutic options are limited. PDAC has one of the most widespread and poorly vascularized desmoplastic stromal responses

of any carcinoma, resulting in tumor hypoxia and nutritional deficiency but no indication of significant cell death (Bergers and Hanahan 2008).

Preclinical studies in PDAC models revealed that hypoxia increases cancer cell proliferation, survival, epithelial-to-mesenchymal transition (EMT), invasiveness, and metastasis, as well as resistance to chemotherapy and radiotherapy, *via* hypoxia-inducible factor (HIF)-1-dependent and -independent mechanisms (Chang *et al*. 2011; Wang *et al*. 2010; Guillaumond *et al*. 2013; Izuishi *et al*. 2000). Recent findings indicate that pancreatic tumor cells adapt to physiologically demanding survival circumstances in their microenvironment (Cohen *et al*. 2015). The activating point mutation of the KRAS oncogene on codon-12 is present in 70–95% of PDAC cases and so far, no success has been achieved to inhibit KRAS. KRAS$^{\mathbf{G12D}}$ regulates cell proliferation, differentiation, apoptosis(Rawla, Sunkara, and Gaduputi 2019). Tumor cells harboring oncogenic KRAS mutations release chemokines (such as granulocyte–macrophage colony-stimulating factor or IL-6) that activate T cells, B cells, myeloid cells (myeloid-derived suppressor cells), and macrophages, which collectively promote the inflammatory response and tumor progression, posing a barrier for emerging creative therapies to penetrate the tumor microenvironment (Hirt *et al*. 2022). Since the KRAS mutations have a significant role from the initiation to progression of pancreatic tumors. Therefore, a targeted approach to block KRAS could have a significant impact in managing the PDAC. But targeting KRAS has not been so far successful and is regarded as undruggable due to the shape and structure of the protein. Recent efforts have been successful in developing a drug, (sotorasib) against KRAS^{G12C} but not KRAS^{G12D}(Hong *et al*. 2020).

Targeting KRAS^{G12D} using siRNAs has been investigated but remains a challenge due to the inefficient delivery/internalization of siRNAs and inhibition of mutated KRAS into the tumor cells. Additionally, KRAS cancers promote pro-tumorigenic immune microenvironment and their cross talk have been seen to stimulate the loss of dependence

on KRAS expression during the course of therapy (Dias Carvalho *et al*. 2019).Therefore, novel combinatorial strategies are required to target $KRAS^{G12D}$ mutation, which can also improve the effectiveness of KRAS inhibition in regressing tumor volume.

2. Statement of purpose

Due to its aggressiveness and susceptibility to anti-cancer drugs, pancreatic ductal adenocarcinoma (PDAC) is one of the deadliest malignancies. Recent preliminary and published studies show high Galectin-1 (Gal-1) levels in both pancreatic cancer and stromal cells, which modulate tumor microenvironment and metastasis. Interestingly emerging studies have shown the undeniable connection between the mutant $KRAS^{G12D}$ and Gal-1. Manero-Rupérez *et.al.* has recently shown that stromal Gal1 is a major modulator of pancreatic cancer formation and progression using c-myc- or KRas-driven animal models of PDAC and genetic depletion of Gal1 knockout in mice. These observed benefits following Gal1 depletion are most likely achieved by a multi-step process including reduced angiogenesis and stroma activation, as well as immune surveillance rescue. Studies suggest that knockout of pancreatic tumors have increased levels of effector T cells CD3+, CD4+, and CD8+ together with decreased levels of CD11b+Gr1+ myeloid-derived suppressor cells, demonstrating that Gal1 overexpressed in PDAC favors immune advantage(Manero-Rupérez *et al*. 2020). These finding have allowed for a newly uncharted territory to be uncovered, where uprising target therapies will be developed, thus providing clinical patients with an addition scope of hope. As a result of these recent discoveries, we believe that concurrent inhibition of mutant K-Ras siRNA and Gal-1 inhibitor would effectively modify the tumor oncogenic network and microenvironment, activating immune cells, repressing pancreatic tumor growth, metastasis, chemoresistance, recurrence, and improving patient life. Therefore, our objective is to develop a novel combination therapy for

PDAC by targeting mutated $KRAS^{G12D}$ and Gal-1 inhibitor together. This will include the delivery of $KRAS^{G12D}$ inhibiting siRNA using superparamagnetic iron oxide nanoparticle (SPION) and the administration of Gal-1 antagonistic inhibitor.

CHAPTER II

REVIEW OF THE LITERATURE

1. Pancreatic ductal adenocarcinoma

1.1. Introduction

Pancreatic Ductal adenocarcinoma (PDAC) is a deadly malignancy with a 5-year survival rate of about 6% (Khorana *et al*. 2016). Surgical resection is a curative treatment option; unfortunately, only 20% of patients have a resectable tumor at the time of diagnosis. Rapid recurrence leads to a five-year mortality rate of 39% in individuals who received surgical resection. In the preoperative care of patients with borderline resectable or locally advanced PDAC, neoadjuvant chemotherapy or chemoradiation therapy has become progressively prevalent. This has allowed for curative surgical resection to be carried on a higher number of patients (Janssen *et al*. 2019). After resection, nevertheless, a significant number of patients have early recurrence or distant metastases. As a result, it is critical to discover preoperative prognostic markers in order to predict long-term outcomes. PDAC is a stroma-rich, vascular-poor, hypo-perfused tumor that results in poor medication delivery, which is the primary cause of treatment resistance (Du *et al*. 2022). Pancreatic ductal adenocarcinoma (PDAC) is the most common type of pancreatic cancer. The transition from preinvasive precursor lesions to invasive pancreatic cancer (Figure 1) takes several years or decades, and parental pancreatic cance normally takes more than 5 years to obtain the ability to invade and metastasis (Yachida *et al*. 2010). The most prevalent antecedents of PDAC are pancreatic

intraepithelial neoplasias (PanINs) (Hruban *et al*. 2001). PanINs are tiny (5 mm in diameter) lesions that are too small to be detected with existing imaging modalities. Individuals with hereditary vulnerability to pancreatic cancer frequently have several PanINs (Koorstra *et al*. 2008; Cooper, O'Toole, and Kench 2013). Various molecular alterations occur throughout the evolution from precursor lesions to PDAC (Guo, Xie, and Zheng 2016). Other variables influencing the fate of this disease include the restricted number of patients who qualify for surgical resection, the insufficiency of currently available detection tools, and less effective chemotherapy therapies(Saxena *et al*. 2022). While surgery followed by adjuvant chemotherapy is typically used to treat local pancreatic cancer, systemic therapies with gemcitabine (alone or in combination) or irinotecan/oxaliplatin/5-fluorouracil combinations are suggested for the treatment of metastatic disease (Tempero *et al*. 2010). Despite tremendous attempts, even the largest phase 3 studies in the first-line metastatic context were unable to achieve an overall survival of more than one year, with response rates ranging from 10% to 30% (Golčić *et al*. 2022).

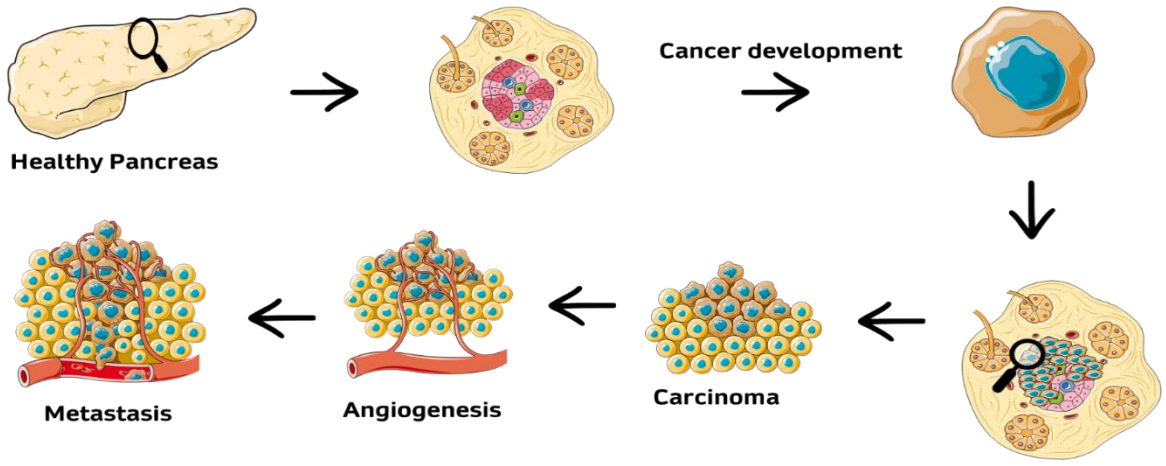

Figure 1. Development and progression of PDAC Pancreatic cancer is thought to be a disease of many genetic changes, and mutations in KRAS/CDKN2A/TP53/SMAD4 increase the development and advancement of precursor lesions.

1.2. Statistics in pancreatic ductal adenocarcinoma cancer

According to the American Cancer Society, PDAC will afflict 62,210 people in the United States in 2022, resulting in 40,560 fatalities with 37,970 being men and 29,240 women. At least 479,773 people will be diagnosed with PDAC worldwide in 2020, 466,003 died. The prevalence of PDACC has grown modestly in the United States, but global instances are expected to rise significantly due to the effect of cigarette smoking, increasing obesity, and type II diabetes.

PDAC is the fourth largest cause of cancer death in both men and women. It is the 11th most prevalent incident cancer in men and the 9th in women (Siegel, Miller, and Jemal 2015). PDAC has an overall age-adjusted incidence rate of 13.9/100,000 males and 10.9/100,000 women (SEER). PDAC is 30% more prevalent in men than in women(Society 2013). At the age of 85, the lifetime risk of PDAC for Caucasians is 1.5 percent (SEER 2021). Incidence rates differ by race, with white males (13.8/100,000) and women (10.7/100,000) having lower rates than blacks PDAC is the fourth leading cause of cancer death in the world, with a five-year survival rate of 10%, the lowest of any cancer kind (Racu *et al*. 2022). According to statistics from the Surveillance, Epidemiology, and End Results Program (SEER) and the National Center for Health Statistics, the incidence of PDAC in men and women increased by 1.4 percent between 2000 and 2009 (SEER 2021) According to the most available SEER statistics (2011/2012), total mortality rates are increasing by 1.7 percent. GLOBOCAN, the International Agency for Research on Cancer, calculates global cancer incidence and death rates(Organization 2012).

In 2012, 337,872 new PDAC cases were recorded worldwide, with 330,372 fatalities.

According to the most recent GLOBOCAN 2012 study, PC has risen to the seventh largest cause of cancer mortality in the globe. For all histological categories, the age-standardized incidence rate is 4.8/100,000 The rates of occurrence fluctuate dramatically between industrialized and developing nations, as well as between men and women. Men have an incidence rate of 8.5/100,000 in highly developed nations and 3.3/100,000 in less developed countries, while women have an incidence rate of 5.6/100,000 in highly developed countries and 2.4/100,000 in less developed countries (Organization 2012).

African-Americans have a greater rate of PDAC (17.6/100,000 for black males and 14.3/100,000 for black women) than other racial and ethnic groupings in the United States (SEER 2021). Asian-Americans/Pacific Islanders have the lowest PDAC incidence rates. Black

Americans are more likely to have advanced illness and are less likely to get PDAC surgery (Chang *et al*. 2005). Death rates for blacks with PDAC are considerably higher: 15.3/100,000 for males and 12.5/100,00 for women (SEER). Excess PDAC risk among American blacks may be linked to race-based disparities in cigarette smoke metabolism, greater levels of cigarette smoking, obesity, excessive caloric intake, heavy alcohol use, long-term diabetes, and low economic level (Silverman *et al*. 2003). Several studies have demonstrated that poor socioeconomic level is associated with a greater stage of PC at diagnosis and worse life expectancy (Silverman *et al*. 2003; Chang *et al*. 2005; Eloubeidi *et al*. 2006).

1.3 Genetic transformation during pancreatic cancer

One of the most important ideas to emerge from more than two decades of pancreatic cancer research is the realization that the illness is caused by both hereditary and somatic mutations. A collection of hallmark mutations characterizes pancreatic adenocarcinoma and distinguishes it from other pancreatic neoplasms (Maitra and Hruban 2008). Almost every PDAC has several numerical or structural chromosomal alterations revealed by cytogenetic analysis due to chromosomal instability, a common feature of most solid tumors (Feldmann and Maitra 2008). Losses on chromosomes 6, 12, 13, and 18, as well as gains on chromosomes 7 and 20, are the most common numerical changes observed in PDAC; chromosomal breaks and rearrangements most frequently occur in regions involving 1p, 1q, 3p, 6q, 7q, 11p, 17p, and 19q (Sirivatanauksorn *et al*. 2001; Griffin *et al.* 1995).

Since 2004, there have been clear guidelines for classifying PDAC precursor lesions, with three distinct types identified: pancreatic intraepithelial neoplasia (PanIN), mucinous cystic neoplasia (MCN), and intraductal pancreatic mucinous neoplasia (IDPMN) (IPMN) (Yachida *et al*. 2010; Kargozaran *et al.* 2011). The PanIN lesion is by far the most common and generic precursor lesion of PDAC. PanINs are found in the smaller pancreatic ducts and are classified into four grades based on the degree of dysplasia reflected in cytonuclear atypia and architectural change: PanIN-1A, PanIN-1B, PanIN-2, and PanIN-3. PanIN-1 lesions have the least severe abnormalities; there is minimal cytonuclear atypia and cell polarity is preserved with a basally located nucleus. PanIN-1A and -1B lesions differ in that the cells in PanIN-1A lesions are flat, whereas the cells in PanIN1B lesions are arranged in a micropapillary architecture (Yachida *et al.* 2010).

PanIN-2 lesions are distinguished by cytonuclear atypia and infrequent mitoses. PanIN-3 lesions, also known as carcinoma-in-situ, exhibit all of the hallmarks of cancer, including loss of polarity, nuclear atypia, frequent mitoses, and lumen budding of groups of cells (Kargozaran *et al.* 2011). The morphological steps of tumor progression that precede invasive PDAC are manifested by increasing grades of dysplasia in the various PanIN lesions (Biankin *et al.* 2004). These sequential steps of tumor progression are genetically accompanied by the accumulation of specific and generalized molecular genetic alterations. PDAC is typically caused by a symbiotic interaction of mutations in tumor-suppressor genes, oncogenes, and genome maintenance genes (Biankin *et al*. 2004). Telomere shortening is presumed to be the initiating event in pancreatic tumorigenesis because it induces genetic instability. Another early event in the development of PDAC is mutation of the oncogene KRAS2, which is altered in 20% of PanIN-1 lesions and increases with progression to invasive carcinoma (Ottenhof *et al.* 2011).

1.4. PDAC mutations

Activating mutations of the KRAS2 oncogene are the most common genetic abnormality in PDAC, occurring in 90–95 percent of cases (Caldas and Kern 1995). KRAS2 encodes a member of the RAS family of GTP-binding proteins that mediate a variety of cellular functions such as proliferation, cell survival, cytoskeletal remodeling, and motility. A variety of stimuli, such as growth factor ligand binding to the cognate growth factor receptor, result in signal transduction *via* intermediary proteins, culminating in Kras protein activation. The active protein binds to GTP and is inactivated by guanosine-triphosphatase-activating proteins, which promote GTP hydrolysis to diphosphate GDP and inhibit Kras signaling. Activating mutations reduce the KRAS2 gene product's intrinsic GTPase activity, resulting in a protein that is constitutively active in intracellular

signal transduction (Caldas and Kern 1995). In pancreatic cancer, the spectrum of KRAS2 gene mutations is primarily limited to alterations in codon 12, with occasional mutations in codons 13 or 61 (Maitra and Hruban 2008).

PDAC is driven by four major genes: KRAS, TP53, CDKN2A, and SMAD4. In PDAC, chromosomal alterations result in the loss of tumor suppressor factors such as CDKN2A, TP53, and SMAD4 (Wu *et al*. 2020). Next Generation sequencing (NGS) analyses of resected PDAC tumors found that KRAS, TP53, CDKN2A, and SMAD4 had the greatest mutation rates, with oncogenic KRAS mutations present in more than 90% of individuals. These findings were corroborated by the International Cancer Genome Consortium (ICGC), which also reported many structural variations. Moreover, The Cancer Genome Atlas (TCGA) database showed the presence of 20 genes altered at a frequency of less than 10%, including chromatin modification genes (including ARID1A, KMT2D, and KMT2C), DNA repair genes (such as BRCA1, BRCA2, and PALB2), and other oncogenes (BRAF, MYC, FGFR1 and others)(Hosein *et al*. 2022). There are four classic mutations among these: KRAS (85%), TP53 (60-70%), CDKN2A (>50%), and SMAD4 (50%). Genes involved in epigenetic control (ARID1A, ARID1B, SMARCA1, MLL2, MLL3, KDM6A) and DNA damage response (ATM, BRCA2) are also mutated, but at a lesser frequency. KRAS mutation is an early occurrence in stage 1 pancreatic intraepithelial neoplasia, according to genetic study of clinical specimens (PanIN) (Luo 2021).

2. RAS and cancer

RAS genes are known as the first mutated genes identified in human cancers(Papke and Der 2017). In this report, we focus on the RAS gene most commonly mutated in human cancers, the KRAS oncogene.

2.1 RAS mutations in cancer

RAS-family proteins are compact 188–189 aa–21 kDa and GTPases having a three-dimensional structure that is extremely similar. These proteins have two domains as well as a core region: The N-terminal G domain (aa 1–165) is highly conserved and consists of a phosphate-binding P-loop, an effector binding domain (aa 32–40), and double switch regions (aa 32–38 and aa 59–76) that are responsible for conformation modifications. The core region (aa 85–165) is shared by 85–90% of the RAS GTPase superfamily. The C-terminal hyper variable region (aa 165–185) regulates membrane attachment and functions as an auto-inhibitory domain. The cysteine residue in the CAAX terminal sequence is farnesylated, facilitating membrane anchoring. Furthermore, the K-RAS4B HVR domain has a lysine-rich region that helps to maintain the protein at the membrane.(Jonckheere, Vasseur, and Van Seuningen 2017) In PanCa,. HRAS, NRAS, and KRAS are all members of the RAS family of small GTPases. These three loci are responsible for the expression of four distinct protein isoforms: HRAS, NRAS, KRAS4A, and KRAS4B. Because of alternative splicing of exon 4 in the KRAS locus, the two KRAS isoforms vary, with KRAS4B being the major isoform expressed in most tissues. Each RAS protein has two primary domains: the G domain and the membrane targeting domain, with considerable changes limited to the hypervariable area of their C-terminal domains(Zeitouni *et al.* 2016). RAS mutations in residues 12, 13, and 61 decrease GTP hydrolysis activity. Although

the three RAS genes are the most frequently mutated oncogene family in human malignancies, the precise isoform and amino acid mutation fluctuates between tumors. Mutations in HRAS are most common in melanoma, bladder, and breast carcinoma; NRAS mutations are most common in melanoma and thyroid carcinoma; and KRAS mutations are most common in bladder, ovary, thyroid, lung, colon, and pancreas malignancies. KRAS is one of the most frequently mutated oncogenes in cancer, KRAS mutation is found in ~95% of PDACs (Bryant *et al.* 2014), KRAS mutation is easily detected in 25% and 38% of PanIN-1A and PanIN-1B patients, respectively(Löhr *et al.* 2005) . Recent data suggests that KRAS mutation is most likely a precursor during early stage in human pancreatic cancer (Luo 2021). Mutations in KRAS codon 12 are the most common in pancreatic cancer (Zeitouni *et al.* 2016). Patients with pancreatic cancer who have KRAS mutations at codon 61 have lower extracellular signal-regulated kinase (ERK) activity compared to patients with other KRAS alleles, and the former have a much better prognosis (Wang *et al.* 2021).

2.2 KRAS gene mutation

Mutated Kras stimulates a number of downstream effector pathways, including the RAF–mitogen-activated protein kinase (RAF-MAPK), PI3K, and RalGDS pathways. RAF-MAPK signaling appears to play an important role in pancreatic carcinogenesis, according to several lines of evidence. One-third of pancreatic cancers with wild-type KRAS2 have BRAF oncogene mutations, resulting in RAF-MAPK signaling activation even in the absence of KRAS2 mutations (Calhoun *et al*. 2003). RAS signaling is based on the active small GTPase RAS, which induces the activation of three key effector pathways. Given that mutations in one RAS protein isoform, KRAS, are identified in almost 90% of pancreatic malignancies, RAS signaling appears

to play a significant role in both the onset and maintenance of pancreatic cancer (Zeitouni *et al*. 2016). When RAS is activated, it can activate effector signaling pathways and transcription factors that are implicated in cell transformation, proliferation, and metastasis. NF-B, signal transducer and STAT3, and glycogen synthase kinase-3/nuclear factor of activated T cell signaling are all activated by activated RAS. Phosphatidylinositol 3-kinase (PI3K), an important protein in apoptosis, is activated by oncogenic K-ras signaling. PI3K activates Akt *via* phosphorylation, which then activates NF-B. The AKT2 gene, which is located on chromosome 19q, is amplified in 10–20% of pancreatic cancers(Cheng *et al*. 1996; Ruggeri *et al*. 1998), whereas PI3K/Akt signaling is activated in roughly 60% of PDACs (Schlieman *et al*. 2003). Mammalian target of rapamycin (mTOR), an Akt downstream target, is also involved in PI3K signaling. mTOR activation has been observed in approximately 75% of PDACs (Bellizzi *et al.* 2010). Pancreatic tumors lacking KRAS mutations demonstrate RAS activation *via* upstream signaling through receptor tyrosine kinases (RTKs), such as: the epidermal growth $KRAS^{G12C}$ RAF) molecule, which is present in a limited proportion of individuals. Despite substantial understanding of the molecular processes of KRAS in many cancer-promoting activities, clinically effective KRAS inhibitors have been difficult to develop, with the exception of a KRAS ^{G12C} (carried by 1.5 percent of pancreatic cancer patients)-selective inhibitor AMG 510.58. In animal models, KRAS inhibition can activate AKT, erb-b2 RTK2 (HER2), platelet-derived growth factor receptor alpha, and EGFR, which could explain why these inhibitors are ineffective (Wang *et al.* 2021).

2.3. KRAS^{G12D}, signaling and its regulation

KRAS activating mutations are found in 95% of pancreatic tumors, while G12 alterations account for 95% of all mutations (G12D—50%) (Cicenas *et al*. 2017). KRAS^{G12D} is the most frequent KRAS mutation, and it is seen in around 34% of pancreatic cancers and 10% to 12% of colorectal cancers, 4% of lung adenocarcinoma, 11% of bile duct carcinoma, 5% of endometrial cancer, and a variety of other cancer types (Christensen *et al*. 2022). KRAS(G12D) is the most common and carcinogenic G12 mutant form, it is estimated to affect more than 50% of individuals with pancreatic ductal adenocarcinoma (Prior, Lewis, and Mattos 2012). KRAS^{G12D} is said to have the second greatest rate of intrinsic GTP hydrolysis among KRAS mutants, as well as the highest rate of GTPase-activating protein (GAP)-mediated GTP hydrolysis (Christensen *et al*. 2022). Cells with KRAS^{G12D} mutations release significant quantities of the anti-inflammatory mediators like, TGF-β and IL10, which are critical chemokines for maintaining an immunosuppressive milieu and cancer cell immune evasion. IL-10 is well-known for inhibiting T cell activation, whereas TGF- suppresses T cell activation and proliferation while also promoting epithelial to mesenchymal transition, which favors cancer cell migration and invasion. Furthermore, pancreatic cancer cells have been shown to block cytotoxic CD8+ T cell-mediated tumor death by releasing IL-10 and TGF- (Pereira *et al*. 2022). J. Tape *et al*. and colleagues show that KRAS^{G12D} communicates with stromal cells non-autonomously *via* SHH-SMO-GLI and renders tumor cells unresponsive to autocrine SHH. Furthermore, KRAS^{G12D} achieves a unique signaling output (e.g., ECM, IGF1, and GAS6) *via* stromal cells that differs from that produced by tumor cell KRAS^{G12D} alone. J. Tape et.al. and team unveils that KRAS^{G12D} controls non-oxidative flux *via* cell-autonomous signaling and mitochondrial

oxidative phosphorylation *via* reciprocal signaling (Prior, Lewis, and Mattos 2012) providing further studies of tumor-stromal crosstalk complex.

In 2003, a significant breakthrough was made with the development of a Genetically Engineered Mice (GEM) that expressed an oncogenic $KRAS^{G12D}$ allele from its endogenous promoter (and thus at physiologic levels) in the developing pancreas *via* Cre-mediated recombination driven by Pdx1 (or Ptf1/p48) regulatory elements (Hingorani *et al.* 2003). Pdx1 is a homeodomain protein that is required for early pancreatic development. In the mature pancreas, both differentiated exocrine and endocrine cell types arise from a Pdx1-expressing progenitor population (Jonsson *et al.* 1994).

3. PDAC tumor immune microenvironment

3.1 KRAS and tumor microenvironment

After noting the presence of leucocytes inside neoplastic tissues, Rudolf Virchow originally hypothesized that cancer begins at areas of persistent inflammation in the 18th century (Balkwill and Mantovani 2001). The function of inflammation in carcinogenesis has been extensively researched and defined during the last two decades (Balkwill and Mantovani 2001). KRAS mutations have been connected to tumor-promoting inflammation and have been identified as a key component in carcinogenesis (Kitajima, Thummalapalli, and Barbie 2016). emerging from organ epithelial linings, specifically the pancreas, colon, and lungs. Oncogenic KRAS produces a number of inflammatory cytokines, chemokines, and signaling pathways that increase tumorigenesis and invasiveness in these tumors (Kitajima, Thummalapalli, and Barbie 2016; Golay and Barbie 2014). KRAS is involved in the beginning and maintenance of PDAC

via a number of processes including its well-established autonomous cancer cell signaling capabilities visually observed in (Dey *et al*. 2020; Hamarsheh *et al.* 2020). KRAS has been demonstrated to influence cytokine receptor expression in cancer cells and invading T cells, which then communicate through JAK1–STAT6–MYC, resulting in glycolysis gene upregulation to enable cancer cell metabolic reprogramming (Dey *et al.* 2020; Hamarsheh *et al*. 2020).

The surrounding extracellular matrix (ECM) has long been linked to cancer progression regulation (for example, migration and invasion). Efforts in the late 1990s and early 2000s focused on non-specific ECMs' change inside the surrounding stroma by targeting proteins that remodel the ECM. Proteolytic matrix metalloproteinases (MMPs) and tissue inhibitors of MMPs were shown to be differently expressed in non-transformed pancreatic and PDAC tissues, with increased expression of certain MMPs linked with metastatic disease and/or a worse prognosis (Bramhall *et al*. 1997; Jones *et al*. 2008; Jones *et al*. 2004; Matsuyama, Takao, and Aikou 2002). MMP2, a type IV collagenase present in the stroma of pancreatic cancer tissues, was reported to promote invasiveness in vitro and to correlate with the degree of desmoplasia (Okada *et al*. 2004; Schneiderhan *et al*. 2007; Jacobetz *et al.* 2013).

Cancer-associated stromal cells (CAFs) are a diverse collection of cells that are known to be key producers of ECM proteins. These generally spindle-shaped cells express one or more activated fibroblast markers (for example, fibroblast activation protein (FAP) and -smooth muscle actin) and have traditionally been linked to various tumor-promoting functions such as tumorigenesis, angiogenesis, immunosuppression, and metastasis, as discussed elsewhere (Chen and Song 2019). Researchers previously demonstrated that cancer-driven signaling *via* IL-1 or TGF may differentiate surrounding fibroblasts into inflammatory CAF and myofibroblastic CAF

phenotypes (Biffi *et al*. 2019). TGF stimulates myofibroblastic CAFs to create the surrounding stroma, whereas IL-6 released by inflammatory CAFs has pro-proliferative effects on the tumor. Following that, a third subtype of CAFs was identified that express MHC class II molecules and may present antigens to CD4+ T cells, suggesting that certain CAFs are involved in shaping antitumor immune responses (Elyada *et al*. 2019). Feig C. *et al*. found that depleting FAP+ CAFs in KPC mice resulted in immunological control of tumor development and a successful response to immune-checkpoint inhibitors (ICIs) (Feig *et al*. 2013). Both investigations demonstrated the relevance of CXCL12–CXCR4 signaling in stromal–immune interaction, offering another therapeutic target (Feig *et al*. 2013).

3.2. Galectin-1 cross talks with KRAS and drives immunosuppressive environment

Galectins are a phylogenetically conserved class of lectins described in 1994 as a common consensus of around 130 amino acid sequences and the carbohydrate recognition domain (CRD) which is responsible for β-galactoside binding (Barondes *et al*. 1994). These galectins have a single carbohydrate recognition domain (CRD) and are physiologically active as monomers (galectins-5, -7, -10), homodimers (galectins-1, -2, -11, 13–14, -15), or oligomers that aggregate through their non-lectin domain (galectin-3), others have two CRDs linked by a short linker peptide (galectins-4, -6, -8, -9, -12). While all galectins' CRDs have an affinity for the minimum saccharide ligand N-acetyllactosamine (a common disaccharide found on many cellular glycoproteins), individual galectins can recognize different modifications to this minimum saccharide ligand, demonstrating the fine specificity of certain galectins for tissue- or developmentally specific ligands (Ahmad *et al*. 2004). Gal-1 was the first protein found in the family. According to the NCBI website's MapViewer application and the Entrez genome

database (http://www.ncbi.nlm.nih.gov/entrez/query.fcgi?db=Genome&itool=toolbar). Gal-1 exists as a monomer as well as a non-covalent homodimer composed of one CRD subunit (Gal-1, 29 kDa) (Barondes *et al*. 1994). Gal-1 may be found both within and outside of cells, and it serves both intracellular and extracellular roles. Gal-1 is a cytoplasmic protein with an acetylated N-terminus and no glycosylations; it has been characterized in cell nuclei and cytosols and also translocates to the intracellular side of cell membranes. Nonetheless, despite the fact that Gal-1 lacks recognizable secretion signal sequences and does not travel through the standard endoplasmic reticulum/Golgi pathway d, it is well-known that it is secreted and can be found on the extracellular side of all cell membranes as well as in the extracellular matrices of various normal and neoplastic tissues.

Gal-1 is found in numerous normal and pathological tissues and seems to be functionally polyvalent, controlling cell proliferation, differentiation, and apoptosis, as well as facilitating tumor transformation and growth. Gal-1 has been shown to be overexpressed in a variety of digestive system malignancies, including gastric cancer, colorectal cancer, hepatocellular carcinoma, and others(Camby *et al*. 2006). Gal1 may attach to Extracellular matrix proteins such as laminin and fibronectin. It is also present in the cell membranes of many different cell types, binding to a variety of receptors such as integrin 51 in epithelial cells, GM1 glycolipid in neuronal cells, and CD45, CD43, and CD7 in immune cells. Gal1 is involved in a variety of cellular physiological tasks, including cell proliferation, migration, adhesion, motility, and T-cell homeostasis.

Using a mix of GEMM and human-based experimental systems, Orozco et.al show that inhibiting Gal1, a protein overexpressed by stromal fibroblasts, may slow PDA tumor development by hindering tumor–stromal crosstalk (Orozco *et al*. 2018).

Using this Kras-driven model, Orozco *et al*. discovered that genetic ablation of Gal1 improves animal survival and limits tumor growth *via* diverse pathways including decreased stroma activation and angiogenesis as well as increased immune cell infiltration (Orozco *et al*. 2018). Furthermore, the team discovered that Gal1 is involved not only in pancreatic tumor initiation but also at late stages of tumor progression(Orozco *et al*. 2018). Gal1 regulates paracrine interactions with epithelial cells to enhance proliferation, migration, and invasion, as well as endothelial and inflammatory cells to increase angiogenesis and immune cell suppression(Orozco *et al*. 2018). Thus, Gal1 controls various molecular signatures and events that are associated with PDAC pathogenesis including tumor cell proliferation, invasion, angiogenesis, inflammation, and metastasis. These studies implicate the extensive therapeutic potential of Gal1-specific inhibitors, either alone or in combination with other therapeutic modalities.

3.3. Galectin-1 signaling, regulation

The LGALS1 gene, which is located on chromosome 22q12, encodes gal-1. The methylation state of the promoter is an important mechanism for controlling gal-1 expression. Gal-1 is a 14 KDa monomer or non-covalent homodimer that has one CRD per subunit. Because the homodimer contains more than one CRD, it can mediate cell adhesion, initiate intracellular signaling, and create multivalent lattices with cell surface glycoconjugates (Astorgues-Xerri *et al*. 2014). Homodimers can connect multiple membrane receptors in the extracellular space, increasing cell signaling and cell–cell interactions and enabling homotypic and heterotypic aggregation (Camby *et al*. 2006; Yang, Rabinovich, and Liu 2008). Gal-1 participates in a variety of physiological processes, including brain stem cell development,

hematological lineage differentiation, and muscle differentiation (Camby *et al*. 2006). Furthermore, compelling evidence accumulated in recent decades suggests that Gal-1 upregulation can significantly influence tumor progression due to its pleiotropic roles in cell transformation (Paz *et al*. 2001), cell proliferation (Camby *et al*. 2006), angiogenesis, cell adhesion and invasiveness, and immunosuppression (Astorgues-Xerri *et al*. 2014). Gal-1 is present intracellularly in the nucleus, cytoplasm, and the inner leaflet of the cytoplasmic membrane (Clerch *et al*. 1988). Gal-1, like the other members of this family, is released into the extracellular space, despite the absence of signaling sequences essential for secretion *via* the conventional endoplasmic reticulum/Golgi route (Hughes 1999). Extracellular Gal-1 has a slightly larger molecular weight (15 kDa) than the 14 kDa version found in cell lysates, indicating that secreted Gal-1 is subjected to additional post-translational changes before or after secretion (Satelli *et al*. 2008). Gal-1 binding, like a receptor-ligand system, may cause intracellular signaling events, for instance, interactions with α5β1 integrin regulates epithelial tumor cell proliferation by inducing p21 and p27 (Fischer *et al*. 2005), activated caspase-8, and sensitized carcinoma cells to anoikis (apoptosis generated by cell anchorage loss) (Sanchez-Ruderisch *et al*. 2011). RAS activation, as defined by GTP binding, is required for the H-Ras/Gal-1 interaction. Extracellular Gal-1 inhibits tumor cell growth in a variety of tumor cell lines, including hepatocarcinoma, melanoma, breast, ovarian, and colon carcinoma, by interacting with 51 integrin, resulting in sustained inhibition of the Ras-MEK-ERK pathway and transcriptional induction of p27, a cell cycle inhibitor. Intracellular Gal-1 interacts with cytosolic or nuclear proteins such H-Ras, FXOP3, and Gemin4 to regulate signal transduction, gene transcription, and messenger RNA splicing (Tsai *et al*. 2022).

3.4 Clinical challenges to target KRAS^{G12D} in pancreatic cancer

KRAS^{G12D} is undeniably a tempting cancer target; nevertheless, there are a number of obstacles that must be addressed in order to efficiently target additional KRAS mutant variations(Christensen *et al*. 2022). KRAS^{G12D}, unlike KRAS^{G12C}, lacks a reactive residue close to the switch II binding region, making covalent alteration to the protein impossible; hence, innovative techniques are required to build selective inhibitors with high affinity and drug-like activity(Christensen *et al*. 2022). Recently, a study showed that KRAS^{G12D}-specific siRNA significantly reduced KRAS expression and suppressed pancreatic tumor development in both subcutaneous and orthotopic mice models (Zeitouni *et al*. 2016). A phase I/IIa clinical trial of si^{G12D}-LODER in conjunction with chemotherapy in patients with locally advanced PDAC was recently completed. The LODER was placed into the tumor *via* a normal endoscopic ultrasound biopsy, allowing it to offer local, ongoing therapy for several months. The medication was well tolerated when combined with FOLFIRINOX, a standard of care chemotherapy cocktail routinely used in advanced pancreatic cancer patients in good health. The combined therapy resulted in a median overall survival of 15.13 months and a median time to metastasis of 8.25 months (Golan *et al*. 2015). Herein, we provide a novelty study for a combined targeted therapy where we are targeting KRAS^{G12D} with a small interference RNA (siRNA) and Gal-1 with an

inhibitor. Additionally, it has been observed that disrupting the MAPK signaling pathway by inhibiting KRAS mutation, increases dependance of pancreatic cancer cells on autophagy to create energy. This reduces the effectiveness of drugs in inhibition of tumor growth. Therefore, this highlights the significance of our study in inhibiting KRAS and Gal-1 together, which will regulate tumor stroma, reprogram immune cells, and prevent autophagic cell response.

CHAPTER III

GENERATION, CHARACTERIZATION, AND FUNCTIONAL CHARACTERISTICS OF A NOVEL SPION-siKRAS + GALECTIN-1 INHIBITOR *IN- VIVO* NANO-FORMULATION FOR PANCREATIC CANCER

1. Background

The most prevalent pancreatic neoplasm is pancreatic ductal adenocarcinoma. It is an invasive mucin-producing gland-forming a tumor that causes a strong stromal desmoplastic response (Kamisawa *et al*. 2016). Pancreatic cancer treatment consists of surgery, chemotherapy, radiation therapy, and palliative care. A multidisciplinary approach is used to identify treatment choices based on the stage of pancreatic cancer; yet, the prognosis remains dismal, with just 20% survival (Mizrahi *et al*. 2020). After being introduced into mammalian cells, siRNA is a short non-coding ds-RNA of 21–23 nucleotides that can induce RNAi silencing without triggering non-specific interferon. It offers the ability to silence genes that encode proteins that are not regulated by small molecules or programmable medicines (Setten, Rossi, and Han 2019). Approximately 90% of PDAC patients have a KRAS mutation, which plays a significant role in PDAC initiation. Kamerkar *et al*. created exosomes from normal fibroblast mesenchymal cells that had siRNA or shRNA to silence $KRAS^{G12D}$ (Kamerkar *et al*. 2017). A Phase I study is now conducted for patients with metastatic pancreatic cancer who have the $KRAS^{G12D}$ mutation (NCT03608631).

Despite the potential of siRNA-therapeutics for cancer treatment, transport of siRNA into cells remains a substantial barrier to clinical usage. This is attributable to (1) the large size of siRNA (about 13.5 kDa) and its negative charge; (2) naked (unmodified) siRNA is susceptible to breakdown by serum proteins in the blood and may be swiftly taken up and removed from the body through the reticuloendothelial system (Xin *et al.* 2017). The capacity of nanoparticles to release siRNA into the cytosol is a crucial physical need that must be carefully considered when creating nanoparticles for siRNA delivery (Kim *et al.* 2016). Fortunately, previous work from mentor's lab demonstrated the production of an innovative superparamagnetic nanoparticles (SPION) for the effective delivery of drugs (Khan *et al.* 2019; Yallapu *et al.* 2011; Khan *et al.* 2014).

Previous magnetic nanoparticle formulations for drug delivery developed by others have shown poor therapeutic effectiveness for cancer therapy due to high particle size in suspension, loss of magnetism, and inadequate internalization in target cells. In contrast, our novel magnetic nanoparticle-based solutions for drug delivery applications are stable and extremely efficient. Our research has shown that our highly advanced SPIONs exhibit multifunctional features, including improved MRI properties as compared to ordinary MNPs (Khan *et al.* 2014; Yallapu *et al.* 2010; Khan *et al*. 2019).

We coupled the SPION formulation with siRNA-KRASG12 in this investigation to obtain pancreatic tumor selective delivery of siRNA-siKRAS. Kras is a member of the highly homologous Ras protein family and has a strong transforming ability. It is a monomeric membrane-localized guanine nucleotide (GTP/GDP)-binding protein with a size of 21 kDa. Kras may be activated by a wide range of extracellular stimuli, and the activated form, in turn, initiates a cascade of signals that eventually govern cell proliferation, differentiation, and death.

Kras mutations are most common at codon 12 (Rachagani *et al*. 2011). As a result, the following three objectives are met in this chapter III: (i) generation and characterization of siKRAS conjugated SPION (SP-siKRAS), (ii) investigation of its ability to internalize efficiently into cells and demonstrate its siRNA targeting ability, and (iii) investigation of the formulation's functional efficacy in combination with Gal-1 inh (inh) using various cell lines, by performing *in-vitro* assays.

2.Materials and methods

2.1 Chemicals, reagents, and antibodies

All chemicals and reagents were acquired from Sigma Aldrich Corporation, while cell culture materials were purchased from Corning Life Sciences. Life Technologies supplied the Trizol reagent (catalog number # AM9738). XenoLight D-Luciferin Potassium Salt (catalog number #122799) from PerkinElmer Health Sciences, Inc. RAS (G12D Mutant) antibody [HL10] was used as the main antibody (Cat No. GTX635362).

2.2 Human pancreatic cancer tissues

Tissue microarrays (TMAs) were obtained from US Biomax, Inc. (Derwood, MD, USA). Pancreatic disease spectrum (pancreatic cancer progression) and pancreas tissue microarray with 42 cases of adenocarcinoma, 2 adenosquamous carcinoma, 1 each of squamous cell carcinoma and islet cell carcinoma, 6 metastatic carcinoma, 10 pancreas islet cell tumor, 11 pancreas inflammation, 21 adjacent normal pancreas tissue and 10 pancreas tissue, duplicated cores per case (PA2081b).

2.3 Scoring of Galectin-1 expression in stained pancreatic normal and cancerous tissues

The slides were digitally scanned and evaluated for Gal-1 staining after histochemical labeling. Captured photos were separately reviewed by three reviewers (Sheema Khan, Radhika Sekhri, and a resident) who were blinded to the patient's history, and a consensus rating was determined. The strength of Gal-1 immunoreactivity was rated on a scale of 0 to 4 (0 for no staining, 1 for mild immunoreactivity, 2 for moderate immunoreactivity, 3 for high immunoreactivity, and 4 for extremely strong immunoreactivity). Within the tumor and neighboring normal tissue sections, the percentage of cells positive for Gal-1 immunoreactivity was graded as follows: 0–25 percent as 1, 26–50 percent as 2, 51–75 percent as 3, and 76–100 percent as 4. The composite score (CS) values ranged from 0 to 16 and were determined by multiplying the staining intensity (0–4) and the percentage of immunoreactive cells (0–4) values for each individual sample. Finally, the mean composite score (MCS) was calculated by taking the average of the composite scores of each category's samples.

2.4 Culture of pancreatic cancer cells

Panc1 and AsPC-1 human pancreatic cancer cells were utilized to test the effectiveness of the SPION-siKRAS nano formulation. In addition, for in-vitro and in-vivo research, we created a lentiviral-expressing KPC luciferase mouse cell line. Pdx1cre; LSL-$Kras^{G12D}$; LSL-Trp53R172H (KPC) mice were used to create the KPC cell line. The KPC mice mimic the progression of the disease in humans, such as PanCa activation with PanINs, progression to invasive adenocarcinoma, and subsequent metastasis to distant organs. The cells have mutations in

transformation-related proteins such as the p53 gene (TP53R172H) and the KRAS gene ($KRAS^{G12D}$).

2.5 Design and preparation of SPION-PEI

By co-precipitating Fe2+ and Fe3+ iron ions in the presence of ammonia in a nitrogen environment, superparamagnetic iron oxide nanoparticles were created. The Fe2+ and Fe3+ iron salts were reduced by ammonia in the presence of 200 mg -cyclodextrin (-CD) and 250 mg Pluronic polymer [(F127, poly (ethylene-co-propylene glycol)], and magnetite formulations were formed as (Figure 2), as a consequence (negatively charged with negative zeta potential values). The CD was acquired from Sigma Aldrich in St. Louis, MO (catalog number # C4805), and it has hydrophilic units (OH) and a hydrophobic cavity for binding to iron oxide nanoparticles and loading anti-cancer medicines, respectively(Khan *et al*. 2019; Yallapu *et al*. 2011; Dan *et al*. 2019) . F127 improves the overall hydrophilicity and stability of the formulation. The nanoparticles were washed three times by placing the water-SPION beaker on a magnet, which separated SPIONs from the water, washing and purifying the nano-formulation Aldrich [408727]. SPION is further conjugated with a third, 25 kDa polymer, polyethylenimine (PEI) Sigma. Polyethylenimines (PEIs) are positively charged, linear or branched polymers that may form nanoscale complexes with small RNAs, resulting in RNA protection, cellular transport, and intracellular release. 2.5mg PEI is added to every 10mg/ml of SPION solution, 2.5mg is added for every 1ml of the SPION (10mg/ml), this formulation is left for 4-6 hours incubating on stirring plate. The formulation is then placed over a magnet for pulling, and simultaneously purifying the formulation. The formulation is now ready to be embedded with siRNA-siKRAS silencer (Figure 3). One hundred nanomolars of siRNA-siKRAS silencer mimics was incubated

with 1 mg/ml of MNP-PEI nanoparticles for 30 min to form SPION-PEI-siKRAS formulation complexes.

2.6 SPION-PEI-siKRAS conjugation

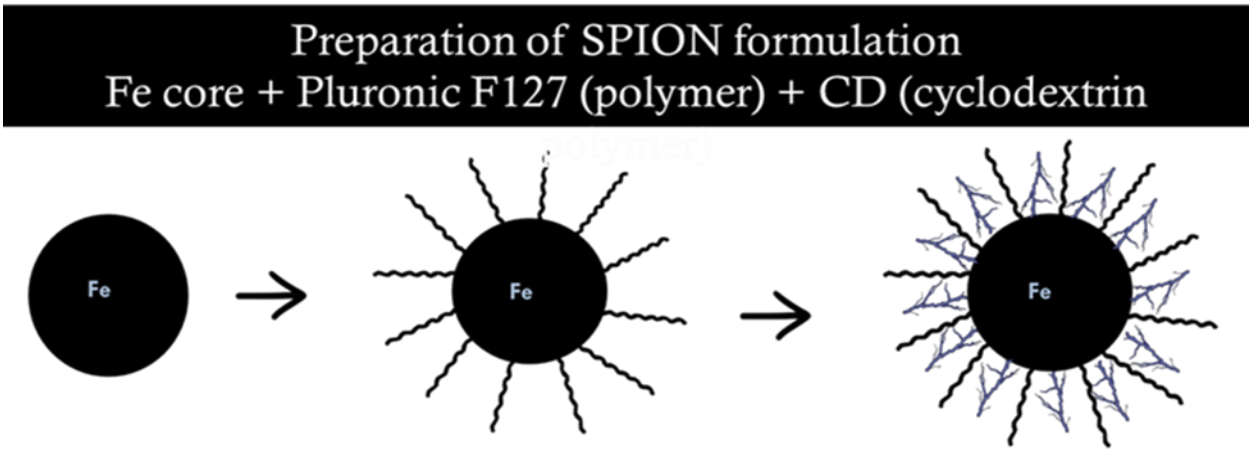

Figure 2. Novel SPION-PEI siKRAS conjugation Final product of SPION (1mg/ml) conjugations containing all three (p-127, CD and PEI) polymers plus conjugation with siKRAS (100 nM). This final step takes 30 min at room temperature.

SPION-PEI-siKRAS (100 nM) conjugation consisted of the dilution of the previously mentioned SPION-PEI stock, where 100:1000 ratio is used to achieve a 1mg/ml desired concentration. An 8ug concentration of SPION-PEI is used per individual treatment, with the addition of siRNA-siKRAS silencer (100 nM) 1ul and 1.5ul of PBS.

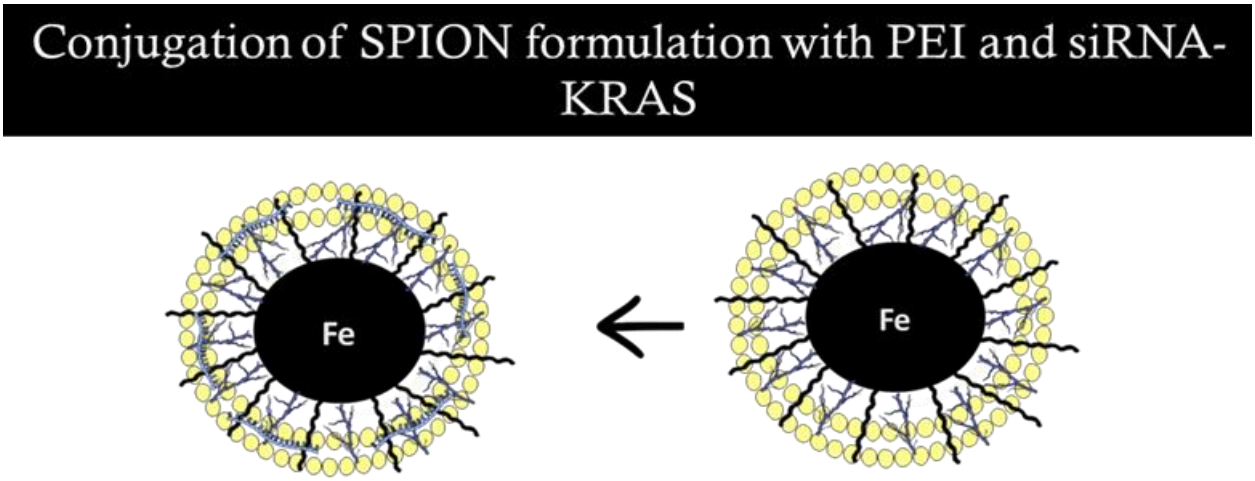

Figure 3. Loading of siKRAS onto SPION SPION particle is used as a delivery system of siKRAS. Diagram depicts conjugation of iron core, F127 polymer, cyclodextrin polymer, addition of PEI polymer

2.7 Determination of particle size and zeta potential of SPION formulation The hydrodynamic nanoparticle size and zeta potential of SPION and SPION-PEI were measured using Zetasizer and the dynamic light scattering (DLS) approach (NanoZS, Malvern Instruments, Malvern, UK). To determine particle size, 150 L of 10 mg/ml nanoparticle suspension was added to 3ml of water and probe sonicated for 15 seconds with VirSonic-Ultrasonic Cell 22 Disrupter 100 128 (VirTis, Gardiner, NY). 50 ul of 10 mg/ml nanoparticle solution was added to 1 ml of 1X PBS for ζ-potential measurement.

3. Internalization of nanoparticle formulation in pancreatic cancer cells

3.1 Prussian Blue Staining for uptake of formulation

Prussian blue staining was used to determine the cellular uptake of SPION formulations in the pancreatic cancer cells; AsPC-1, Panc-1 and KPC. Cells were seeded in a 24 well plate with 50 thousand cells per well and the next day cells were treated with no SPION, SPION-siKRAS, Gal-1 inh (5 uM), and SPION-siKRAS + Gal-1 inh (5 uM) in ASPC-1 and PAnc-1 cell lines. SPION, SPION-siKRAS, Gal-1 inh (5 uM), and SPION-siKRAS + Gal-1 inh (5 uM) on KPC cell line. After 6hrs, cells were washed (with 1X PBS), fixed (with methanol), and incubated with a mixture of 2%potassium ferrocyanide, 2% hydrochloric acid (30 min).

3.2 Confocal immunofluorescence assays for cell internalization

SPION-CUR internalization was studied in pancreatic cancer AsPC-1, Panc-1, and HPAF II human cell lines, as well as KPC lines. Cells were treated with an SPION-PEI-siKRAS nanoparticle formulation and immunofluorescence was used to assess internalization, which was then observed using confocal microscopy. SPION, SPION-siKRAS, Gal-1 inh (5uM), and SPION-siKRAS + Gal-1 inh (5uM) was administered to cells in a 24 well plate (50,000 cells/well) for 24 hours. Cells were trypsonized and re-seeded in an 8-well chamber or a 4-well chamber slide for 12-16 hours after 24 hours of incubation. The treatment was terminated and fixed with 4% PFA for microscopy to produce immunofluorescence images. For immunofluorescence tagging, antibodies against Gal-1 and $KRAS^{G12D}$ (RAS (G12D Mutant) antibody [HL10] Cat No. GTX635362) were utilized.

3.3 Gel retardation assay

The complexes were produced for the gel retardation analysis by adding 100 nM siKRAS to 1–10 g nanoparticles (SPIONs), vortexed immediately, and allowed to stand for 30 minutes. The complete binding process was carried out in a 20 µL solution. Gel electrophoresis was performed on complex solutions using 2 percent agarose gel in the presence of an agarose gel ladder. The gels were then stained for 20 minutes with 0.5 g/mL ethidium bromide and studied on a UV illuminator (UVPTM Multi-User Imaging System, Upland, CA, USA) to determine the mobility or location of the siRNA-siKRAS complex.

3.4 Internalization of formulation in clinically relevant cell line models, spheroids

Cells were seeded in a 24 well plate and incubated for 24 hours. To create primary spheroids, cells were seeded in a 96 well ultra-low attachment plates and allowed to develop for 7 days. the re-location of the spheroids from a low-attachment 96 well plate to a low-attachment 6 well plate which allowed secondary spheroids to form on an ultra-low attachment surface.

4. Anti-Cancer efficacy of SPION-siKRAS formulation in pancreatic cancer cells

4.1 Viability assay

In this study KPC (50,000/well) cells were seeded in a 24 well plate and treated accordingly (control, SPION-siKRAS, Gal-1, SPION-siKRAS + Gal-1). Cells were incubated for 24 hours. Cells were then trypsonized and counted for viability using a CountessTM Automated Cell Counter in a trypan exclusion study. Cell viability was evaluated as a ratio of treated to untreated cells.

4.2 Spheroid assay

Primary tumor spheroid was developed using KPC and Panc-1 or ASPC-1cell line. This assay mimics the tumor microenvironmental condition and we investigated the effect of SPION-siKRAS and Gal-1 inh (alone and in combination), properties in spheroid formation ability. Cells were seeded in a 24 well plate and incubated for 24 hours. To create primary spheroids, cells were trypsonized and re-seeded in a 96 well ultra-low attachment plate and allowed to develop for 7 days. the re-location of the spheroids from a low-attachment 96 well plate to a low-attachment 6 well plate allowed for the formation of secondary spheroids on an ultra-low attachment surface (Corning) in DMEM/F12 (KPC), DMEM (Panc-1) and RPMI (ASPC1) complete medias (10% fetal bovine and 1% anti-mycotic-anti-microbial) and treated them with previously mentioned treatment groups for 5-7days. After one-week primary spheroids were photographed and compared with the size of SPION (control).

4.3 Wound healing

Cell migration was analyzed using wound healing assay, as described before (Khan *et al*., 2015). Cells were seeded in a 24 well plate (50,000/well) treated with SPION, SPION-siKRAS, Gal-1 inh (5uM), and SPION-siKRAS + Gal-1 inh (5 uM) and incubated for 24 hours. cells were then trypsonized and seeded in 24 well plate with 65,000 cells per well to form a monolayer. Next day cell monolayer was scraped using a 200µL micropipette tip and tin KPC cell line (mouse) and Panc-1 (human). After 48hours-72 hours of treatment the residual gap length was captured as described earlier(Yallapu *et al*. 2015). The plates were photographed for migrated cells using phase contrast microscope at day 0hrs, 48hrs, and 72hrs.

4.4 Boyden chamber migration assay

The impact of SPION, SPION-siKRAS, Gal-1 inh (5uM), and SPION-siKRAS + Gal-1 inh (5uM) on KPC and Panc-1 cells was investigated using 96 well insert migration Chambers (BD Biosciences), according to the manufacturer's procedure. Cells were starved overnight with FBS negative medium and counted the next day. Cells were seeded in a 24 well plate (50,000/well) treated with SPION, SPION-siKRAS, gal-1 inh (5u M), and SPION-siKRAS + Gal-1 inh (5 uM) and incubated for 24 hours. Cells were then trypsonized and counted. In FBS-free medium, 35,000 cells were re-seeded into the top chamber. While the lower chamber received FBS-positive media. The migratory cells were fixed with methanol and stained with crystal violet after 12- 18 hours of incubation. The migratory cells were captured as migration of SPION-siKRAS, Gal-1 inh (5 uM), and SPION-siKRAS + Gal-1 inh (5 uM) treated cells compared to control (SPION).

4.5 Matrigel invasion assay

To study the impact of SPION-siKRAS on KPC cells, a cell invasion test was done using BD Biocoat Matrigel Invasion Chambers (BD Biosciences) (Yallapu *et al*. 2015) (HAVING TROUBLE WITH CITATIONS) according to the manufacturer's protocol. Cells were seeded in a 24 well plate (50,000/well) treated with SPION, SPION-siKRAS and incubated for 24 hours. Cells were then trypsonized and re-seeded in the upper compartment 40,000 cells in FBS negative medium, whereas the bottom chamber was planted with 40,000 cells in FBS positive media. The invading cells were preserved with methanol and stained with crystal violet after 24- and 48-hour incubations. Invaded cells were collected as invasion of SPION-siKRAS treated cells were compared to the control.

5. Molecular analysis of SPION-siKRAS and Galectin 1 inhibitor in pancreatic cancer cells

5.1 Real-time PCR

TRIZOL reagent was used to extract total RNA from HPAF, Panc-1, and KPC cell lines (catalog number AM 9738, Invitrogen). Gene expression was normalized to GAPDH, and the fold change for SPION-siKRAS, Gal-1 inh and SPION-siKRAS + Gal-1 inh were measured and plotted on a graph. Total RNA from the KPC and Panc-1 cell lines were utilized to investigate the degree of SPION-siKRAS and Gal-1 gene expression.

6. RESULTS

6.1 Galectin-1 expression is increased in human PDAC tissues with the progression of pancreatic cancer

To determine the relationship between Gal-1 and clinicopathological parameters, patient samples were grouped and analyzed for Gal-1 positivity based on sex (78 males and 89 females), age (141 patients with age 50 and 68 with age >50), and TNM staging (27 individuals with tumor located to pancreas and 34 with extension beyond pancreas) (Figure 4). Gal-1 positive was shown to be substantially associated with advanced stage development into neighboring organs or metastasis to lymph nodes (N0-N1); N0-N1 (MCS N0=8.75 Vs N1-N1= 7.25; p= 0.3196), T2, T3, T4 (MCS T2=8.67 Vs T3=8.3 p= 0.7290 Vs T4= 8.33 ; p= 0.8331), Grade (MCS G1=5.94 Vs G2=9 p= 0.0029 Vs G3= 10.63; p= 0.0001), Gender (MCS F=8.80 Vs M=8.98; p= 0.7801), Stage (MCS I=9.22 Vs II&III=8.53; p= 0.3814) and Age (MCS >50=8.18 Vs <50=9.23; p= 0.0400).

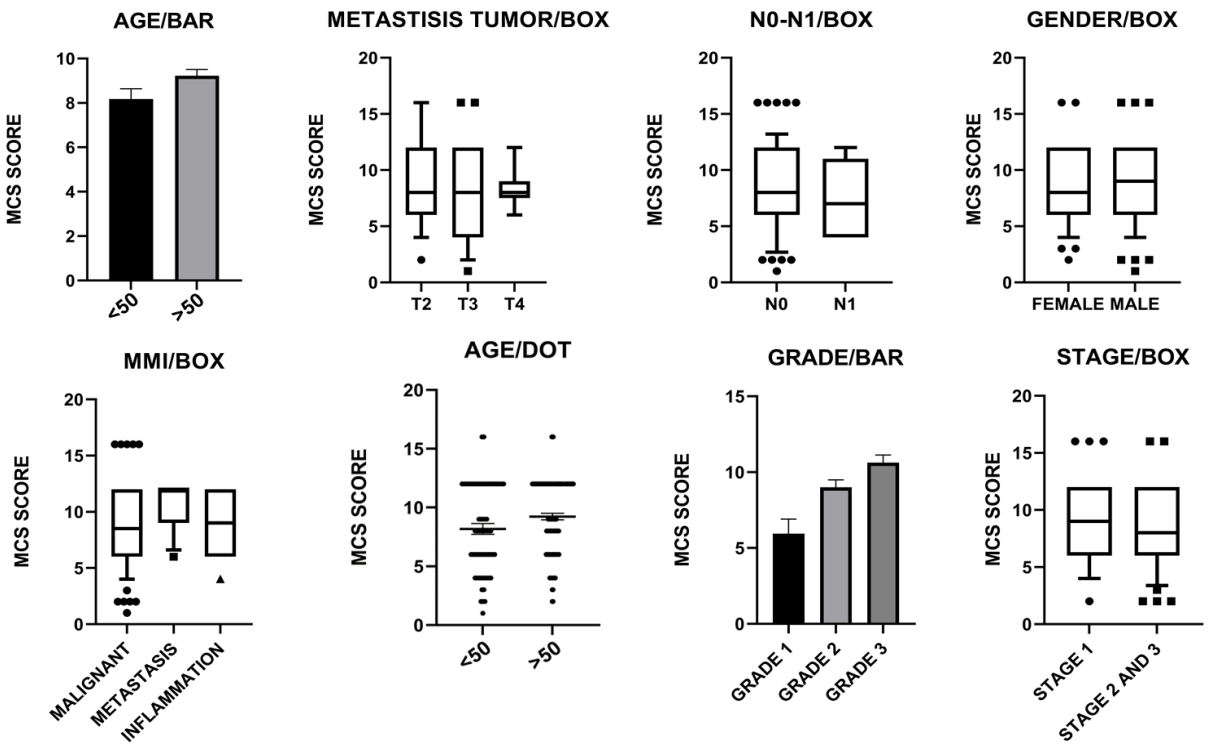

Figure 4. Expression of Galectin-1 in PDAC Pancreatic microarray tissue slide was used to stain it with Gal-1 antibody, then it was scored with Mean Composite Score parameters. The information was then organized in different groups for further analysis. The groups created to investigate age, metastasis tumor, regional lymph nodes, gender, distant metastasis, Age, Grade, and stage.

6.2 Galectin-1 expression is observed in human PDAC cells

Confocal immunofluorescence was performed as described earlier. Cells were fixed and incubated with rabbit anti-Gal-1 antibody for 1 hr. Localization of Gal-1 was analyzed by further incubating cells with Alexafluor-cy3 fluorophore mouse mAb as secondary antibody and nucleus was stained with DAPI. Images were captured for DAPI (blue) and gel-1 (red) in pancreatic cancer cells (Figure 5). Gal-1 expression is present in all cell lines tested (BXPC3, HPAF II, Mia Paca and KPC). KPC cells show a higher expression of Gal-1 when compared to other cell lines implemented.

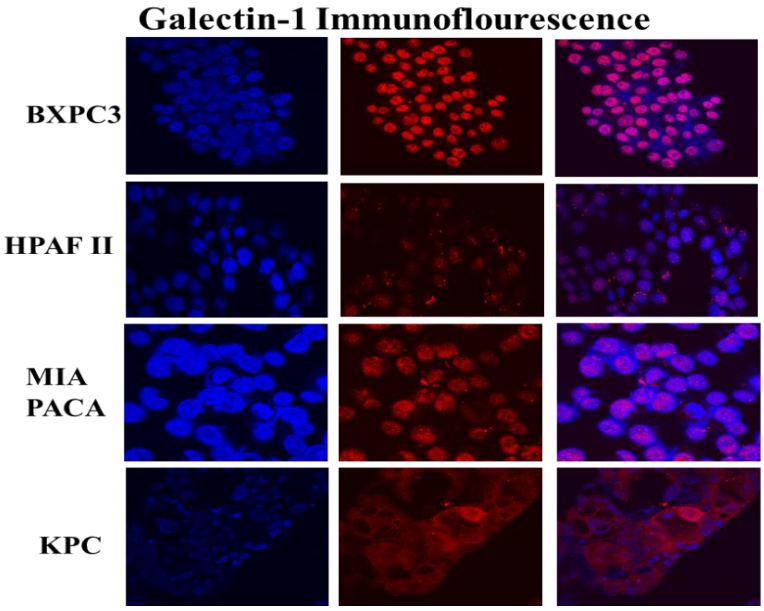

Figure 5. Galectin-1 expression of cell lines through immunofluorescence staining

Gal-1 expression was tested on human cell lines, BXPC3, HPAF II and, MIA PACA, and mouse cell line, kpc

6.3 Successful generation of SPION formulation for pancreatic cancer

PDAC has a dense tumor microenvironment, which makes medication administration extremely difficult. Previous work by mentor's lab reveals the effectiveness and administration of a unique SPION with exceptional characteristics. The researchers devised a multi-layer method for producing water-dispersible superparamagnetic iron oxide nanoparticles for hyperthermia, magnetic resonance imaging (MRI), and drug delivery. In this method, iron oxide core nanoparticles were created by precipitating Fe ions in the presence of ammonia, and they were coated with -cyclodextrin and pluronic polymer (F127). This formulation (F127250) is extremely water dispersible, allowing the anti-cancer medication(s) to be encapsulated in -cyclodextrin and F127 polymer for prolonged drug release. When compared to pure magnetic nanoparticles, the F127250 formulation demonstrated better hyperthermia effects over time in an alternating magnetic field (MNP) and β-cyclodextrin coated nanoparticles (CD200). PEI was employed as a cationic polymer to improve SPION-siKRAS surface attachment. The dynamic light scattering approach was used to determine particle size and charge. SPION-PEI was effectively prepared and stabilized using polymers -cyclodextrin, F-127, and PEI, as shown in Figures 2 and 3, and then coupled with $KRAS^{G12D}$ silencer siKRAS for pancreatic $KRAS^{G12D}$ mutant targeting. In order to determine the core weight, we lyophilized the formulation using a lyophilizer equipment. Every time, an average of 7- 10 mg/ml was achieved, and this formulation could be kept at 4°C for two weeks. Prior to each treatment, new batches were created. The weight of the iron core was estimated using the empty tube technique, which measured the weight of the tube with and without lyophilized nano formulation.

6.4 SPION-siRNA complexation with nanoparticle

The gel retardation experiment was used to investigate the complex formation of MNPs with siRNA-siKras silencer (ambion AM 51334) at varied ratios. For 30 minutes, MNPF (1–10 g) was incubated with 100 nM siRNA-siKRAS mimic. Gel electrophoresis was done using a 2 percent agarose gel that was allowed to run for 1 hour at varied time intervals before photographing the gel to assess particle mobility. In Figure 6, we can observe from left to right at 0 the siRNA-KRAS^{G12D} silencer easily traveling down the gel, whereas, comparing it to 1-8 where different concentrations of SPION were used. Optimal concentration observed was at 8 µg of SPION at well 8.

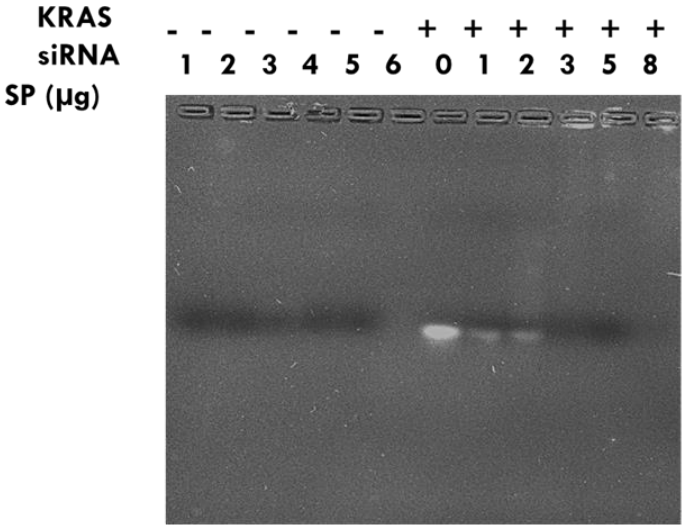

Figure 6. Successful complexation of SPION with si-RNA-KRAS^{G12D} silencer Agarose gel electrophoresis gel retardation experiment demonstrating the creation of a complexation between SPION and the siRNA-siKRAS silencer via electrostatic contact. Complex formation is observed in lane 3, and complexation develops further in lanes 5 and 8 when MNP concentration (1, 2, 3, 5, and 8ug) increases

6.5 SPION-siKRAS was observed to have an optimal size and charge

SPION-siKRAS delivery success is dependent on its size and charge. The Zetasizer machine was used to assess the size and charge of the SPION before and after loading silencer siKRAS. The size of the nano formulation was assessed by dissolving 150 l of nano formulation in 3 ml of pure water, repeating three times, and calculating the average. Our formulation has an optimal average size range for SPION of 96.76-112.5 nm and 115.9-122.6 nm for SPION-PEI-siKRAS. By dissolving 50l of the nano formulation in 1ml of 1X PBS, the formulation's charge was evaluated; a preferred negative charge was achieved for both SPION and SPION-PEI-siKRAS (Figure 7). The formation's average zeta potential was -23.8 - -28.2 mV for SPION and 19-23.2 mV for SPION-PEI-siKRAS (Figure 7)

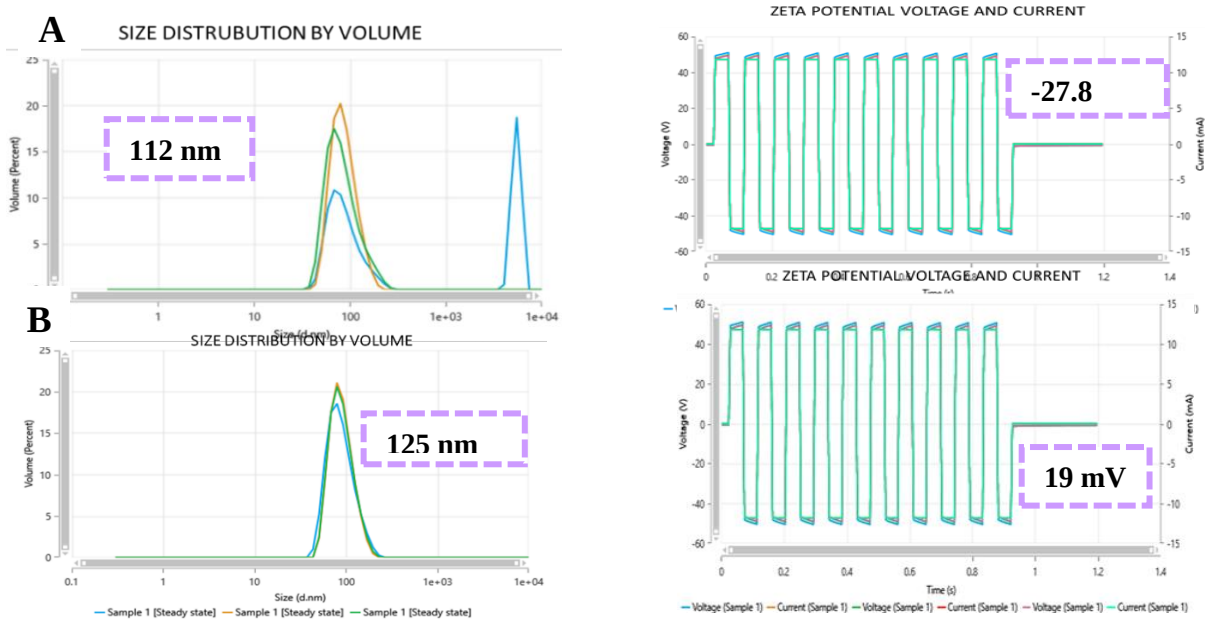

Figure 7. SPION-PEI-siKRAS nano-formulation characterization Graphs exhibiting the size and charge distribution of (A) SPION and (B) SPION-PEI-siKRAS nano formulations using Zetasizer. The size distribution by intensity was measured in nanometers, and the formulation's zeta potential was recorded in voltage

6.6 siKRAS formulation internalized efficiently in the pancreatic cancer cells

We investigated the formulation for its efficacy in cell internalization using various procedures. We found that the formulation in internalizing the cells efficiently using various procedures:

6.7 Prussian blue

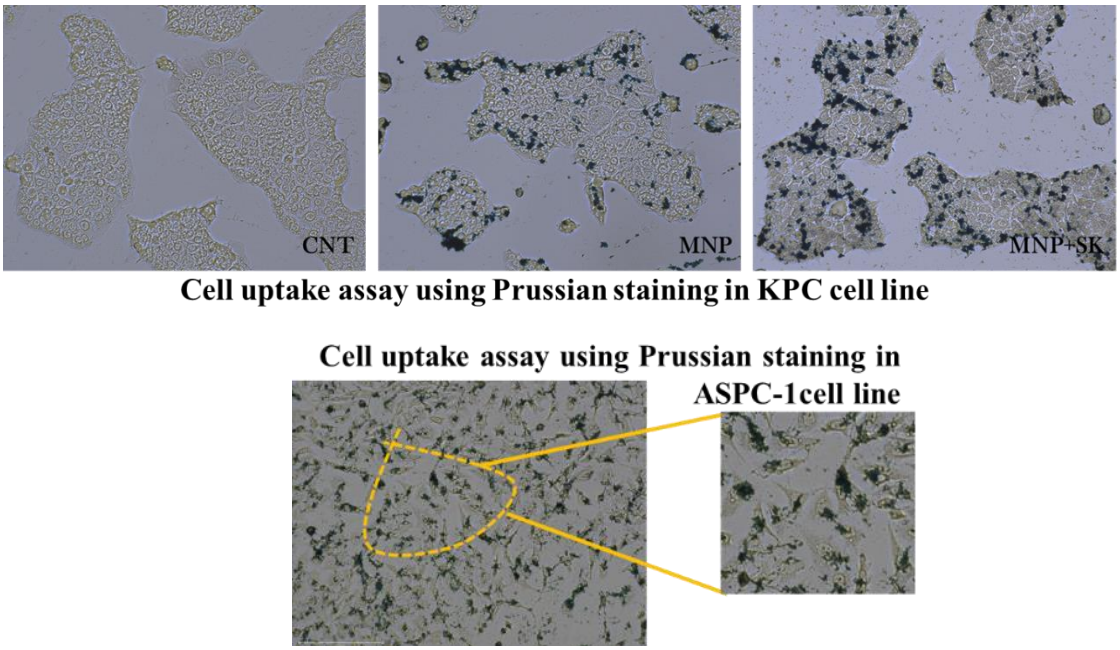

Figure 8. Internalization of SPION-siKRAS Prussian blue staining was used to internalize the SPION-siKRAS nano formulation. After 6 hours of incubation, Prussian staining was used to test the cell uptake effectiveness of SPION(SP), SPION-PEI, and SPION-PEI-siKRAS in (A) KPC and (B) ASPC-1 cell lines.

Prussian staining is one approach for determining iron particle absorption in cells. This staining technique detects the presence of iron in the cell, then reacts and produces a blue hue as a signal. Prussian blue was used to stain the SPION and SPION-siKRAS groups, which may be seen as dark blue dots created by ferric to ferrous iron reduction (Figure 8). The findings at 16-18

hours (human) and 24-48 hours (mice) clearly show the existence of nanoparticles within the cells. Nanoparticle uptake was constant in pancreatic cancer cells, demonstrating that these particles are adaptable and may successfully deliver therapies.

6.8 Immunofluorescence

The complexation efficiency of the SPION-PEI-siKRAS formulations and fluorescein amidite (FAM)-labeled siRNA was determined using fluorescence quenching (the FAM label provides fluorescence). Above, on figure 9 We can observe the individual DAPI staining of the nucleus and the specific staining of the conjugation SPION-PEI-siFAM labelled (KRASG12D). The siRNA formulation was observed SPION-PEI-siFAM was let to conjugate for 30 minutes before administrating to cells. Once concoction is administered a 16-18 hrs incubation period takes place. Cells were fixed and stained with primary antibody KRASG12D (GENETEX 132480) for an hour. The samples were then incubated for an hour with secondary antibody Alexafluor-488 (light sensitive). Samples were washed and mounted then stored at 4°C.

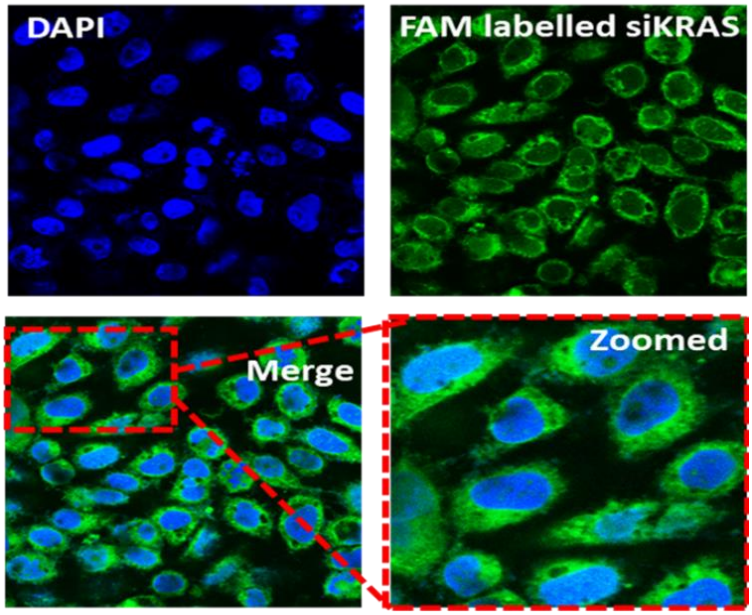

Figure 9. Internalization of SPION-siKRAS through immunofluorescence Dapi staining was used to stain the nucleus of ASPC1 cells, SPION-siKRAS, tracked and, located through siFAM labeled (AMBION)

6.9 Treatment of combined SPION-siKRAS + Galectin-1 inhibitor reduces PDAC cell growth

We investigated the therapeutic potential of inhibiting KRAS and Gal-1 (Gal-1) together in PDAC cells. The SPION-siKRAS formulation was given in conjugation to Gal-1 inh PDAC cells and investigated for the efficacy of co-targeting genes using procedure illustrated below.

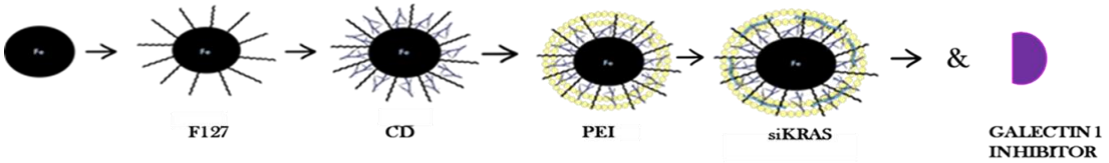

Figure 10. Novel therapy treatment SPION-siKRAS + Galectin-1 inhibitor SPION conjugation is needed prior to treatment (30 min). Once SPION-siKRAS formulation is successful, Gal-1 inh (DB21) is added to the cocktail prior to treatment with a 5 µM

6.10 Inhibition of proliferation, growth, and migratory ability of PDAC primary and secondary spheroids

Primary spheroids are a useful in-vitro 3D model for testing the anti-cancerous activity of SPION-siKRAS. The formulation's capacity to suppress spheroid development was studied as it is a most clinically relevant experiment to evaluate the therapy for potential against clinical samples. Cells were separated into four groups and treated as follows: control, SPION-siKRAS, Gal-1 inh, and SPION-siKRAS + Gal-1 inh for the formation of spheroids. The number of spheroids generated and the size in the presence of therapy was calculated for each treatment group (Figure 11 upper group, left). The spheroids were allowed to grow as secondary spheroids without treatment in an ultra-low attachment plate to investigate the potential of sustained inhibition of PDAC cells by combined treatment (Figure 11 upper group, right). These findings also show that SPION-siKRAS + Gal-1 inh therapies inhibited the formation of primary tumor spheroids when compared to SPION-PEI (control) and SPION-siKRAS in KPC cells (Figure 11 lower group, left). The primary spheroids were allowed to grow as secondary spheroids and reseeded in a non-ultra-low attachment plate to observe the effect of treatments on migratory properties.

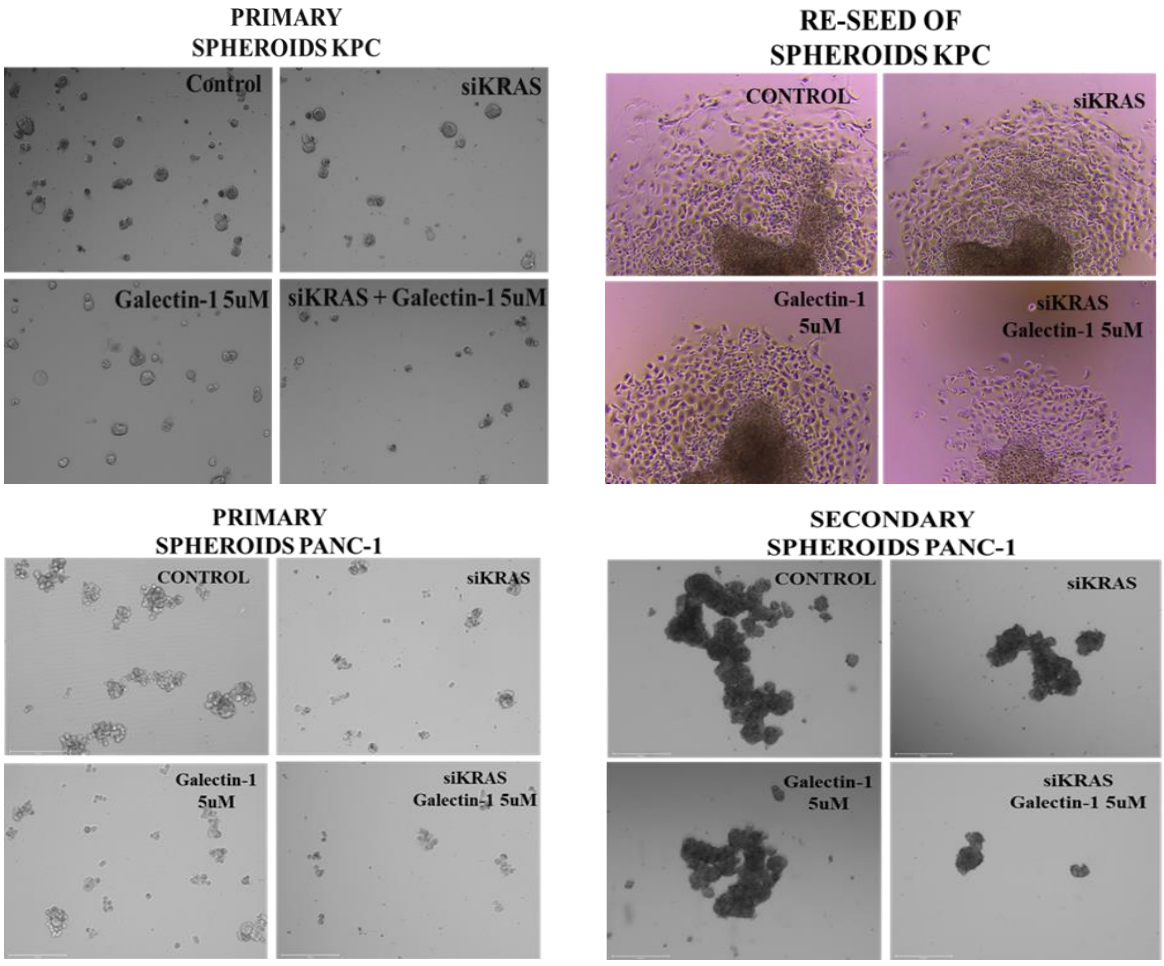

Figure 11. Spheroid formation post-treatment Spheroid assay was conducted in Panc-1 cell line **(Upper panel)** treated with control, SPION-siKRAS, Gal-1 inh 5 µM, and combined **(left)**. Spheroids were then re-seeded into a low attachment tissue culture plate (corning) where analysis was done on cellular migration away from spheroid **(right)**. Spheroid assay was also conducted in KPC mouse cell line **(Lower panel)** and investigated for the effect of treatment on primary spheroid **(left)**, and the migratory ability of cells of secondary spheroids upon seeding them in non-ultra-low attachment plates **(right).**

Our results show that SP-siKRAS combined with Gal-1 inh treatment can successfully penetrate the PDAC cells and inhibit tumor growth.

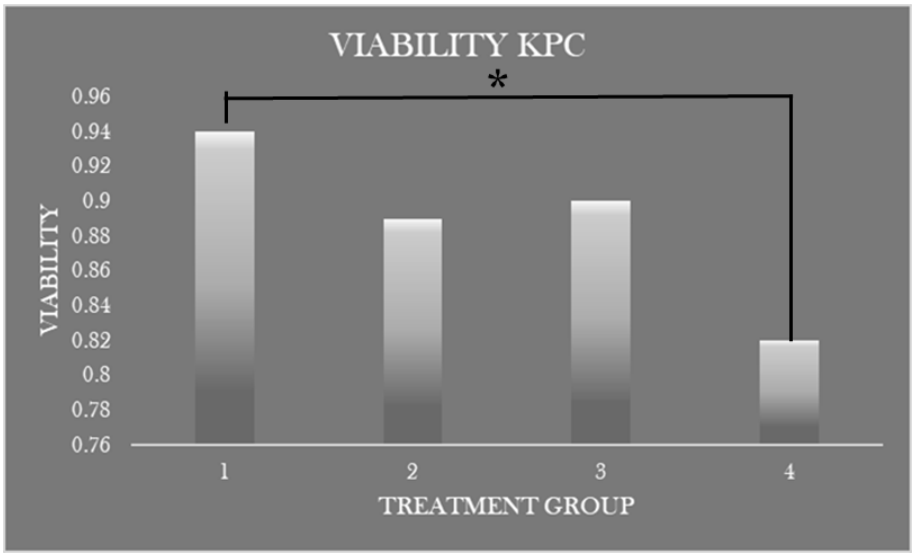

Figure 12. SPION-siKRAS, Galectin-1 inhibitor 5 µM, and combined viability assay KPC (treatment groups): 1 control, 2 SPION-siKRAS, 3 Gal-1, and 4 SPION-siKRAS + Gal-1 this difference is considered to be statistically significant. With a P value of 0.0068, by conventional criteria, this difference is very statistically significant.

6.11 The combined effect of SPION-siKRAS and Galectin-1 inhibitor shows inhibition in PDAC cell proliferation

The proportion of viable cells in KPC cells was determined using a cell viability test. Following 24 hours of incubation, live cells from each group were counted using an automatic cell counter (Invitrogen Cell Countess), and the percentage of viability gained from counting was utilized to produce the graph (Figure 12). The percentage viability of KPC cell lines reduced after treatment with formulations. Following our methodology, the % cell viability of treated samples after incubation was determined in comparison to the preceding control.

6.12 Wound healing assay depicting inhibition of migratory ability in PDAC upon treatment

Wound healing assay is a molecular approach that uses the creation of a wound in cells to evaluate cell migratory capacity that can lead to wound closure. Wound healing assay was used to investigate inhibition of migratory ability in PDAC cells due to combined treatment of SPION-siKRAS + Gal-1. The cell migratory capacity of KPC (Figure 13 A) and Panc-1 (Figure 13 B) discovered to be decreased by SPION-siKRAS + Gal-1 inh therapy, as shown in Figure 13 The initial (0hr) and residual gap lengths at 24 and 48 hours after wounding were measured and recorded. Before each image was captured, cells were rinsed with 1X PBS. The control SPION-PEI demonstrated close to or full wound closure, but the treatment groups all had different healing patterns. When comparing the SPION-siKRAS + Gal-1 inh gap combinatory therapy to

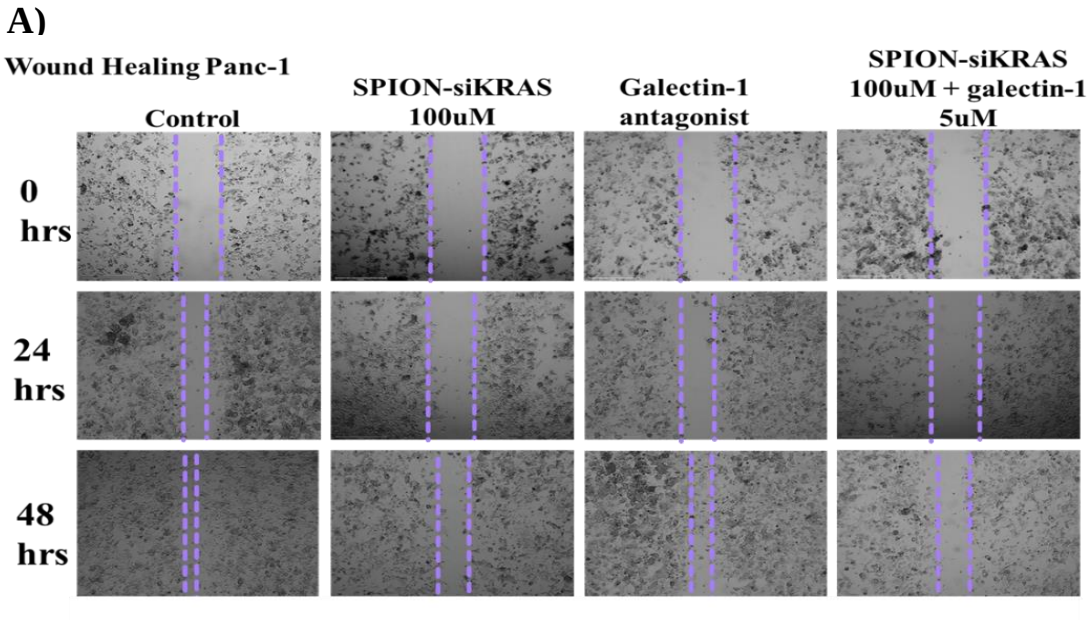

Figure 13. Wound healing The wound healing test was used in this investigation to determine the therapeutic effectiveness of SPION-siKRAS, Gal-1 inh 5 µM, and SPION-siKRAS plus Gal-1 inh.

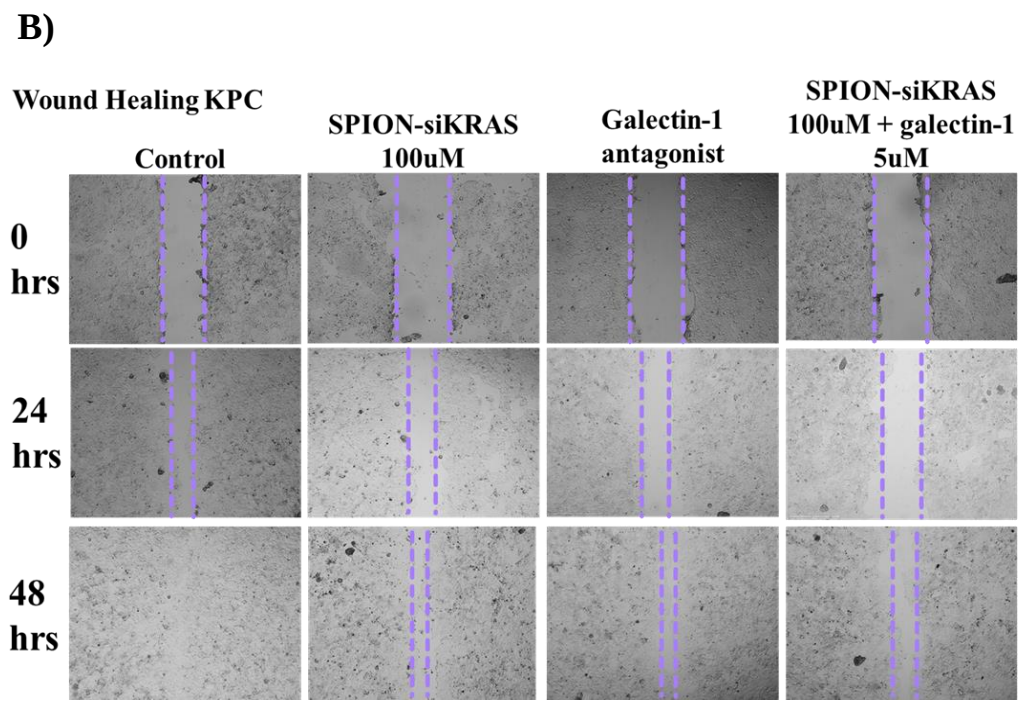

Figure 13, cont. Wound healing was used to test the capacity of Panc-1 **(A)** (human) and KPC. **(B)** (mouse) cells to mend after a wound was generated. KPC and Panc-1 cells were treated for 48 hours, and images were taken at 0hr, 24hr, and 48hr

any of the other groups focusing mainly on the control and SPION-siKRAS groups we can observe a predicted response.

6.13 SPION-siKRAS + Galectin-1 inhibitor reduces invasion and migration in PDAC cells

The invasiveness and migration of KPC and Panc-1 pancreatic cancer cells were studied, and pictures were captured and analyzed. Cancer cells have the ability to invade and migrate towards media containing FBS chambers, a characteristic known as chemotaxis. The ability of KPC and Panc-1 cells to invade after treatment (SPION-PEI, SPION-siKRAS, SPION-siKRAS+Gal-1 inh) reduced with treatment groups. Treatment group of SPION-siKRAS + Gal-1

inh reduced the number of invading cells, indicating that SPION-siKRAS + Gal-1 inhibits KPC, and Panc-1 cell migration (Figure 14 A). Similar findings were obtained in a invasion experiment, which revealed that increasing the concentration of SPION-siKRAS + Gal-1 lowered the number of migrating cells (Figure 14 B).

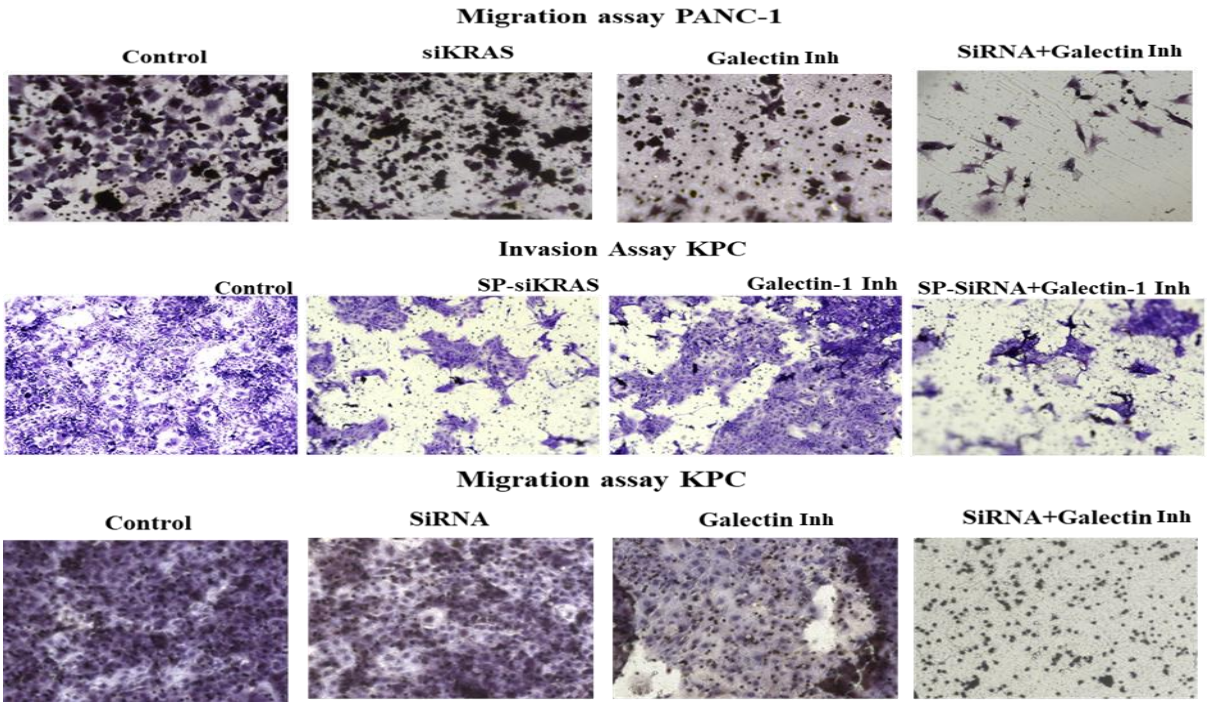

Figure 14. Boyden chamber migration assay and Matrigel invasion assays in KPC and Panc-1 cells Therapeutic efficacy study of SPION-siKRAS + Gal-1 on migration using Panc-1 cells and KPC cell line and invasion using KPC cells. The crystal violet staining the blue color depicts the cell invasion and the hematoxylin staining the red color depicts cell migratory ability of KPC after treatment.

6.14 SPION-siKRAS and Galectin-1 inhibitor reduces tumorigenic features of pancreatic cancer cells

Using real-time PCR, we sought to observe if SPION-siKRAS + Gal-1 inh therapy changes the expression of KRAS and Gal-1 in KPC and Panc-1 cells. Significant alterations in the expression of both KRAS and Gal-1 were found as shown in Figure 15. Overall, our findings on the KPC cell line back up our initial notion. When compared to the control (SPION-PEI), both siKRAS-SPION and Gal-1 inh treatments showed a reduced fold change. Additionally, expression of mutant $KRAS^{G12D}$ was investigated in all cells with high expression in HPAF-II, which was not considered for further experiments due to low Gal-1 expression as shown above.

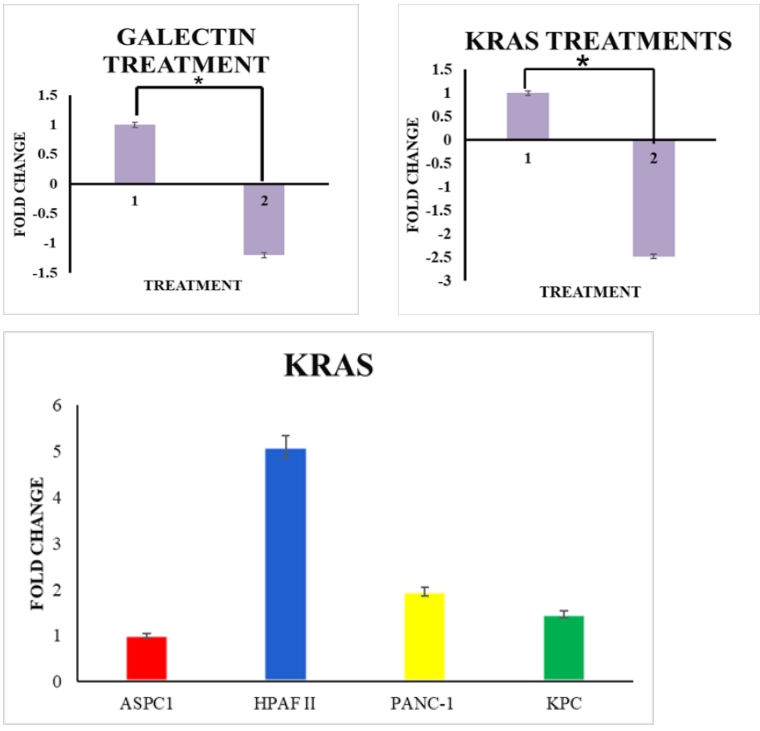

Figure 15. PCR quantification of Galectin-1 inhibitor and KRAS Was performed on PanCa cell lines after treatment with Gal-1 inh and SP-siKRAS, simultaneously (upper panel). The $KRAS^{G12D}$ expression was observed in all PDAC cells (lower panel).

7. Discussion

Because of late detection and the development of chemo-resistance, pancreatic cancer (PanCa) is the third highest cause of cancer-related fatalities in the United States (Yallapu *et al*. 2013). SPION particles generated in this investigation are based on patented particle formulation (Yallapu *et al*. 2013), which allows for improved delivery of silencer siRNA-KRAS^{G12D} in cell lines. Our novel nano-formulation SPION-siKRAS allows the targeting of mutated KRAS^{G12D} which successfully inhibits KRAS^{G12D} mutation. The study reported here attempts to create an effective therapeutic for people with advanced pancreatic cancer. A combination of a stroma inh and a superior tumor targeting technique will be implemented in this study. Gal-1 is overexpressed in PanCa, which promotes cancer metastasis, proliferation, tumor transformation and migration. Unlike other cancer types, PanCa is extremely resistant to chemotherapy medications due to desmoplasia and a fibrotic tumor microenvironment (TME), making it critical to develop alternative treatment techniques for the effective delivery of treatments that are particularly targeted to the tumor site. In this study we demonstrate how to use a unique technique to selectively target and deliver medicines to the pancreatic tumor location.

In this chapter we have generated a novel nanoparticle formulation of SPION-siKRAS. To deliver it, we have generated a novel nanoparticle formulation of siRNA-KRAS-SPION for the delivery of siKRAS silencer therapeutically to the tumors. Per this novel therapy we have used three polymers for the stabilization of the particle pluronic F127, beta cyclodextrin, and polyethyleneimine (PEI) and the conjugation siRNA-SPION.

We have then furthered our study by adding a Gal-1 inh (antagonist) to the already concocted SPION-siKRAS to investigate their functionality, the effects of the inh and KRAS silencer together and their response to PDACs aggressiveness. This formulation is significantly

inhibiting the proliferation, migration, ability to formulate spheroids, and gene expression of the cells.

This formulation is important, and promising, inhibiting both could lead to the re-programming of the TME. Using a Gal-1 inh and at the same time being able to inhibit $KRAS^{G12D}$ mutation using SPION-siKRAS will not only aid in migration, invasion, and tumor cross talk but it will silence KRAS mutation. We are furthering this study by studying the efficacy of the combination treatment of SPION-siKRAS + Gal-1 inh using a pre-clinical synergetic mouse model. This model, known as the $KRAS^{G12D}$; Trp53 R172H; Pdx-1Cre (KPC), C57BL/6J mice (specific to this study)

8. Conclusion

The results show that SPION-siKRAS + Gal-1 inh has a high therapeutic importance for attaining targeted pancreatic tumor specific therapy administration. Because SPION-siKRAS particles inhibit KRAS mutation, Gal-1 in conjunction with SPION-siKRAS has the potential to limit tumor growth, progression, transformation, migration, and invasion by halting tumor-stromal crosstalk (NEXT CHAPTER IV). This study has the potential to improve patient survival.

CHAPTER IV

IN-VIVO AND *EX-VIVO* STUDIES USING NANO-FORMULATIONS FOR PANCREATIC CANCER THERAPY

1. Background

We recommend the reader to numerous recent studies that address in detail the creation of these models, which integrate mutations in proto-oncogenes (e.g., KRAS) and tumor suppressor genes (e.g., TP53, SMAD4, and CDKN2A) that are particularly targeted to the mouse pancreas (Pérez–Mancera *et al*. 2012; Westphalen and Olive 2012). The KRAS proto-oncogene and the TP53 tumor suppressor gene are two of the most frequently altered genes in PDAC (Hruban *et al*. 2001; Jones *et al*. 2008; Biankin *et al*. 2012; Waddell *et al*. 2015). KPC mice reacted in the same way as human patients when treated with typical PDAC therapy techniques(Lee *et al*. 2016). A variety of genetically modified mice models of pancreatic cancer have recently been reported and validated. Hingorani *et al*. identified one paradigm in which mutant KRAS expression and concurrent p53 deletion, especially in the mouse' pancreas, result in pancreatic intra-epithelial neoplasia (PanIN) lesions that proceed to invasive ductal adenocarcinoma (Hingorani *et al*. 2005). This model, known as the $KRAS^{G12D}$; Trp53 R172H; Pdx-1Cre (KPC) model, is one of the most extensively utilized for understanding pancreatic cancer pathophysiology (Majumder *et al*. 2016). The latter form, known as KPC mice, is the most promising preclinical model of PDAC at the moment (Lee *et al*. 2016). In this study in a

syngeneic Orthotopic xenograft mouse model, we aim to analyze the therapeutic efficacy of our innovative nanomedicine technique. For the planned research, we employed a KPC mouse-generated cell line (LSL-KrasG12D; LSL-Trp53R172H; Pdx1cre) to create a syngeneic orthotopic xenograft mouse model of PDAC. These cells are produced from the Pdx1cre; LSL-Kras^{G12D}; LSL-Trp53R172H (KPC) transgenic mouse model, which is a promising preclinical animal model for studying the progression and development of PanCa growth and metastasis. This is because they mimic the disease process found in humans, which begins with mPanINs, progresses to invasive adenocarcinoma, and then metastasizes to distant organs. The experiments were carried out using C57BL/6 wildtype mice. As a result, KPC mice will give a unique opportunity to study the impact of our hypothesized SPION-siRNA-K-Ras^{G12D}-SPION formulation on PanCa development and metastasis in an unmodified animal model (Figure 16)

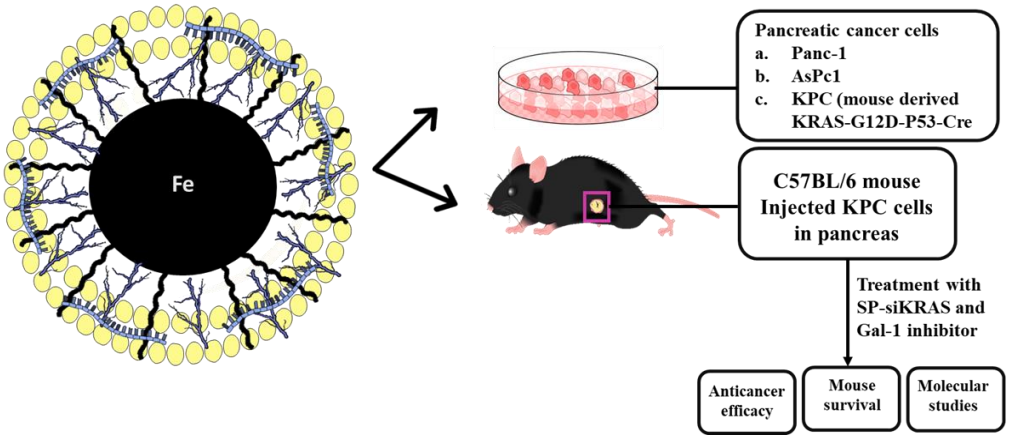

Figure 16. Schematic representation of proposed study Gal-1 is used in combination with SPION-siKRAS on combinatorial effects. Treatment of cells and mice with SPION formulation siKRAS-RNA and Gal-1 inh have been used for functional significance of the combined treatment for *in-vivo* assays.

2. Materials and methods

2.1 Chemicals, reagents, and antibodies

Sigma Aldrich Corporation (St. Louis, MO, USA) provided all chemicals and reagents, while Corning Life Sciences provided cell culture materials (Tewksbury MA, USA). Ly-6CmAb (47-5932-82), CD8amAb (# 15-0081-82), Ly-6GmAb (61-9668-82), CD27mAb (# 11-0271-82), CD45mAb (# 67-0451-82), CD4mAb (# 61-0042-82), CD25mAb (# 35-0251-82), F4/80mAb (# 62-4801-82) BIO-X-cell immune checkpoint antibodies, and polyclonal human IgG (#BE0092). Solution for tissue storage (MACs medium, lot number 130-100-008).

2.2 Stable transduction of luciferase gene in KPC cells for bioluminescence

Cells were grown in DMEM/F12 (Gibco) media supplemented with 10% fetal bovine serum (Gibco) and 1% antibiotic and antimycotic solution at 37°C and 5% CO2 incubator with 95% air environment. In the lab, stable lentiviral luciferase cells, KPC were maintained. To summarize, the cells were treated with a variety of antibiotic dosages to identify the lowest dose that kills all the cells. Pre-packaged viruses were used for lentiviral transduction. XenoLight (PerkinElmer #122799) was used to measure luciferase activity every two weeks.

2.3 Animal handling survival surgery in C57BL/6J mice

Female C57BL/6J mice aged 8 weeks from Jackson Laboratories were utilized in animal experiments. The University of Texas Rio Grande Valley Institutional Animal Care and Use Committee authorized and evaluated all protocols (UTRGV-IACUC: AUP-20-15).

2.4 Pancreatic cancer cell line preparation for implantation

KPC was utilized to create cells that consistently expressed lentiviral luciferase. These transduced pancreatic cancer cells were grown until they were 70% confluent and vitality were better than 90%. The cells were resuspended at 1 x 106 cells/ml in a cold Matrigel: Phosphate buffered saline mixture. The KPC cell line is known to develop quickly, this cell number is only a reference and may vary depending on the cell line. Mouse preparation: A mouse was anesthetized by inhaling 2-3 percent isoflurane. The level of anesthesia was evaluated by the absence of a pedal reaction in response to a mild toe pinch. To avoid desiccation, lubricant was administered to the eyes. The mouse was placed on its back on a 37 ℃ heating pad, and the mouse was gently moved to lift the left side of the abdomen. The abdomen was swabbed with a 10% povidone iodine solution.

2.5 Laparotomy

A 1.5 cm incision was made in the skin approximately 1 cm left lateral from the midline with a sterile surgical tool. The procedure is then followed by a 1.5 cm incision in the underlying abdominal muscle. The spleen was carefully removed from the abdominal cavity using forceps. To reveal the underlying pancreas, the spleen was tethered using a sterile cotton bud, the pancreatic tail was identified close to the spleen and the underlying pancreas was gently removed from the peritoneal cavity for a brief moment. We administered 20 µl of the Matrigel-cell solution into the pancreas using a 29 G 0.3 ml insulin syringe. Following the injection, we hold the syringe in the pancreas for 30-60 seconds to allow the Matrigel to solidify. This is a critical

step that can help to reduce cell leakage. The injection site was examined to ensure there was no leaking. The spleen and pancreas were surgically re-implanted into the abdominal cavity.

2.6 Abdominal wall closure

The mouse's abdominal musculature was closed using an absorbable braided 4-0 suture and a round needle using a continuous stitch. Following that, 1-3 staple(s) per mouse were utilized to close the external skin using non-absorbable staples. After removing the mouse from the inhaled anesthetic, 0.05-0.1 mg/kg meloxicam was administered subcutaneously (30 ul). For recuperation, the mouse was put on a 37 °C heating pad with unrestricted access to food and water. Meloxicam was administered to mice every 12 hours for 36 hours if they showed indicators of discomfort, such as hunching or restricted movement; mice's respiratory patterns and capacity to respond to touch were observed. Every 15 minutes, mice were turned from side to side until they could sustain sternal recumbency. During daily health checks, mice were observed for any changes in behavior, such as anorexia, aversion to movement, and so on. The indicated dose of analgesics was administered as needed. Any animal that had an unfavorable response or received an incorrect injection was withdrawn from the research and euthanized. All mice were observed for tumor development and general symptoms of morbidity such as ruffled fur, stooped posture, and immobility after tumor implantation.

2.7 Preparation of formulation and treatment strategy

All SPION formulations have been conjugated with PEI. The mouse model developed a tumor five days after implantation, mice were then sorted adequately. These assortments were done for four different treatment groups which were comprised of five mice per group: Group1- SPION (1mg/ml) in conjugation with scramble siRNA (100 µM) and 1.5 µl of PBS per mice; Group 2- SPION-siKRAS (100 µM), 0.9% NaCl (4 µL/mice), and 1 µl of PBS per mice; Group 3- Gal-1 inh DB-21 (Sigma Millipore (Sigma-Aldrich 505823) was suspended in PBS and stored (-20°C) in 1mg/ml working stock, a 5 µM concentration was administered as treatment per mice. Each dose had an addition of 1:1 PBS dispersant respectively; Group 4- SPION (1mg/ml)-siKRAS (100 µM), [0.9% NaCl (4 µL/mice), and 1 µl of PBS per mice] plus, Gal-1 (5 µM) and a total dispersant volume of 216 µl (PBS) for entirety of the group (N=5). SPION formulations weighing 100 g/mice and Gal-1 inh treatments were administered intraperitoneally twice a week (Mondays and Thursdays) for four weeks into each mouse group. Every week, mice were imaged, while their deaths remained tracked. The tumor and tissues were dissected, collected, and stored properly for further molecular assays.

2.8 Flow cytometry

2.8.1 Tissue dissociation and preparation of single cell suspension. Tumor tissue kept in MACs tissue storage solution was used to make a single cell suspension. Tumor tissue was sliced into 2- 4mm pieces and put to a mild MACs C tube with an enzyme mix (Tumor dissociation kit protocol #). Gentle MACsTM octo dissociator with heating and enzymatic treatment was used to create single-cell suspensions with great prbility and a high degree of uniformity for repeatable findings. MACS® Tissue Dissociation Kits are intended to recover large quantities of viable single cells with intact epitopes from virtually any solid tissue. To guarantee that the influence on all cell types collected from the tissue sample was limited, a red blood cell lysis solution was utilized. One liter of cell suspension was diluted with ten volumes of 1X RBC lysis solution. (For instance, mix 1 mL of cell suspension with 10 mL of 1XRBC cell lysis solution.) The cells were vortexed for 5 seconds prior to getting incubated at room temperature for 2-3 minutes, ideally 5. After incubation, cells were centrifuged at 300 X g for 10 minutes at room temperature and the supernatant was discarded.

2.8.2 Staining of cell suspension. Centrifugation at 350 Xg for 7 minutes at 4°C rinsed the cell pellet with 1ml of 1X PBS. Following washing, cells were resuspended in 1ml of 1XPBS and counted. The cell density was adjusted to 1 x 106 cells per 1 ml fluid. 1 µl of reconstituted fluorescent reactive dye was added and thoroughly mixed in. Component A (fluorescent reactive dye) was created by combining it with component B. (anhydrous DMSO). For 30 minutes, cells were incubated at room temperature. (Caution: light sensitive.) Wash the cells with 1X PBS after incubation by centrifuging them at 350 Xg for 7 minutes at 4°C and discarding the supernatant. A 100 µl volume of supernatant residue was saved.

2.8.3 Fixation and permeabilization of cell suspension. After adding 100 µl of IC fixation buffer and vortexed the mixture, the cells were fixed. Fixed cells were incubated at room temperature for 35 minutes (Note: Light sensitive). Following incubation period, the cell suspension was washed twice with 1ml of 1X PBS at 450 Xg for 5 minutes at room temperature. The supernatant was removed, and the cell pellet could be stored at 4°C for 2-3 days in 5% FBS and 95 % 1X PBS. After staining the fixed cells with cell surface markers, they were permeabilized with 1X permeabilization buffer. For flow analysis (1 million cells/flow), the cell antigen was resuspended in flowcytometry staining buffer. Two antibody panels were immune profiled for each of the four therapy groups. F4/80, CD11b, CD45, CD27, CD44, Ly6G, CD8, CD45RB, CD3, Ly-6C, and CD25 antibodies are included in the first panel, and FOXP3, CD4, CD25, and CD3 on the second panel. The flow cytometer Attune was used for the analysis.

2.9 Animal handling and survival surgery in C57BL/6J mice

In this investigation, a mouse pancreatic cancer cell line, KPC luciferase (0.2 x 106 cells/ml) in a 1:1 combination of cooled Matrigel:Phosphate buffered saline was employed. Luciferin has been transfected into these cells for bioluminescence imaging of animals. C57BL/6J mice (8 weeks old) will be divided into the following groups and injected orthotopically with mouse pancreatic cancer cells (suspended in 50 µl PBS) using the following techniques, followed by medication treatments through intraperitoneal route. Surgery was a success, all mice were properly handled pre, during and post-surgery. Closing of incision Mice were observed carefully after surgery, during recovery period. Over the next couple of days mice were closely monitored, especial attention was needed for area of incision, which resulted in proper care and manipulation (Figure 17). Prior to treatment all incision were properly healed, and staples were removed.

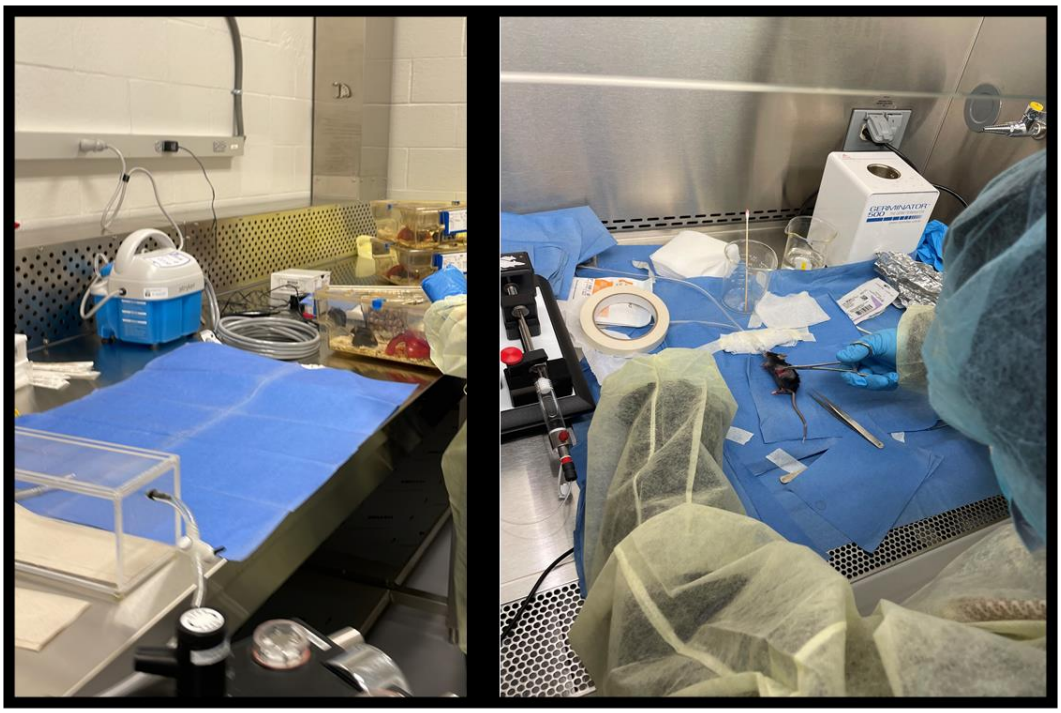

Figure 17. Set up during surgery day Surgery Day (March 8th, 2022) began with the preparation of the surgery room. Equipment set up, turned on, sterilization of surfaces and equipment. Female C57BL/6J mice were used in this study. Area of incision was properly shaved and sterilized prior to surgery. Surgery was done inside a fume hood with proper air flow and proper UTRGV procedure were implemented.

2.9.1 Treatments. The model developed tumor within a week and sorted randomly for 4 treatment groups (N= 5), which include, Group 1: SPION-si-scrambled (control), Group 2: SPION-siRNA-KRAS^{G12D}, Group 3: Gal-1 inh, Group 4: SPION-siKRAS + Gal-1 inh. Treatments started at day 6 after surgery (n=5 mice per group). Drug treatments were administered through intraperitoneal route (Figure 18); Group 1: SPION-si-scrambled (control) (100 nM), Group 2: SPION-siRNA-KRAS^{G12D} (8 µg SPION, 100 nM siKRAS), Group 3: Gal-1 inh (5 µM), Group 4: SPION-siKRAS + Gal-1 inh 8ug SPION, 100 nM si-KRAS, 5 µ M Gal-1 inh. Treatments were administered twice a week (Monday and Thursday intraperitoneally). Mice were monitored for death on a daily basis with the support of UTRGV Edinburg Animal House team. Test subjects were dissected where the tumor and organs were collected for further molecular studies. Tumors were extracted, cleaned, weighed, and measured accordingly.

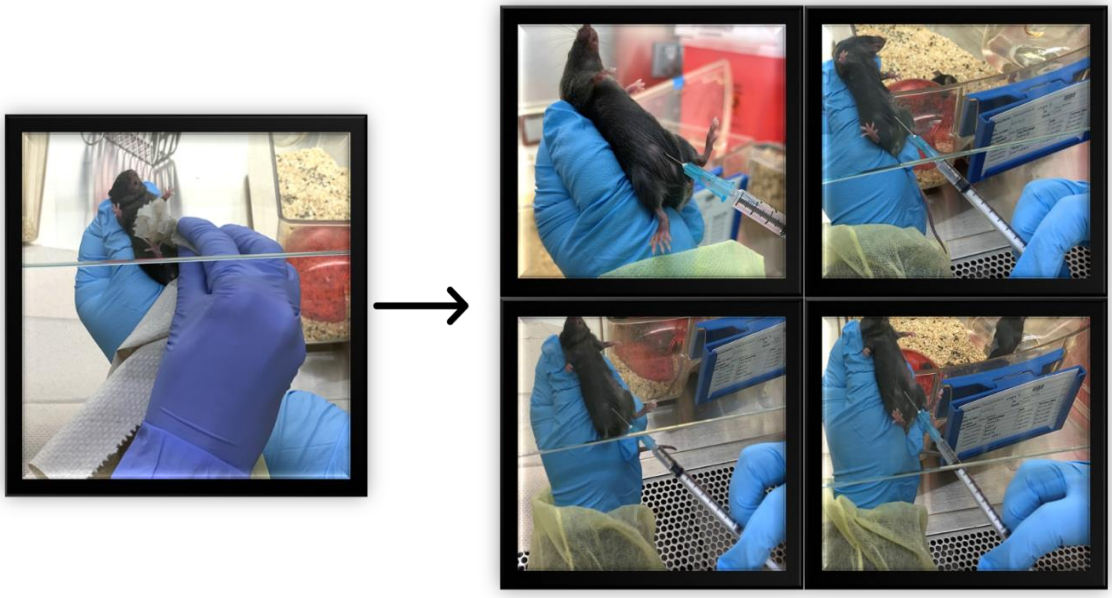

Figure 18. Treatment Mice were segregated according to tumor size into four groups: control (si-scammbled), SPION-siKRAS, Gal-1 inh, and SPION-siKRAS + Gal-1. Mice were handled with proper care. Area of treatment administration was sterilized before and after.

3. Results

3.1 Culture and maintenance of luciferase expressing KPC cells for bioluminescence

The KPC cell line is a well-established and important model for investigating pancreatic ductal cells. We cultured these cells to generate a syngeneic orthotopic xenograft mouse model of PDAC utilizing C57 black mice and KPC mouse derived cell lines (LSL-$KRAS^{G12D}$; LSL-Trp53R172H; Pdx1cre) (Figure 19). The KPC mouse model mimics human disease development, such as PanCa start with mPanINs, progression to invasive adenocarcinoma, and subsequent metastasis to distant organs. It has a point mutation in the transformation related protein 53 gene (TP53R172H) and a non-functional KRAS gene ($KRAS^{G12D}$). Metastases are seen in 80 percent of KPC mouse models, particularly in the lung and liver. As a result, orthotopic mouse models with KPC cancers will be useful for studying both localized and metastatic malignancies. The cells exhibited exceptional bioluminescence as measured by a plate reader (Figure 19). When these KPC luciferase cells are implanted into the pancreas, they can follow tumor development and metastasis, allowing us to establish the effectiveness of the treatment. KPC luciferase was cultivated on a wide scale and its luciferase activity was determined using PerkinElmer's XenoLight substrate.

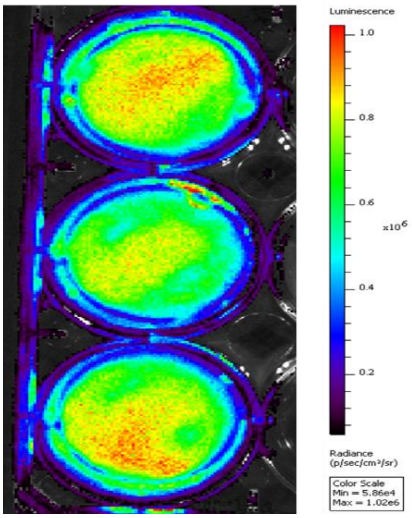

Figure 19. Bioluminescence imaging in KPC luciferase cells Luciferase activity of KPC luciferase cell was tested using XenoLight Bioluminescent/Chemiluminescent Substrates PerkinElmer. Normal KPC mouse pancreatic cell was used a control.

3.2 SPION-siKRAS + Galectin-1 inhibitor combination treatment had no effect on tumor weight in -*KRAS^{G12D}; LSL-Trp53^{R172H}* syngeneic mouse model of PDAC

Five days after cell implantation, mice were randomly sorted into five groups and began receiving treatments as described in Material and Methods section. At this moment we observed the difference in weight when comparing prior to surgery and four weeks after surgery. We can observe a slight increase in weight. We can conclude that mice weight increase is due to the advancement of PDAC causing inflammation and weight gain.

Surgery Day (grams)						Average
GROUP 1 A	18.7	21.8	20.53	20.75	18.72	20.1
GROUP 2 B	17.9	18.3	18.1	18.17	18.47	18.188
GROUP 3 C	18.5	20	20.34	19.3	21.07	19.842
GROUP 4 D	20.52	19.67	17.3	18.78	18.36	18.926

Four Weeks after Surgery (grams)						Average
GROUP 1 A	23.7	20	19.4	22.5	20.4	21.2
GROUP 2 B	20.6	19.9	20.7	19.2	21.3	20.34
GROUP 3 C	18.76	20	22.5	21.8	23.1	21.232
GROUP4 D	22.2	17.9	21.4	22.1	20.5	20.82

Table 1. Mice weight prior to surgery and pre-euthanasia Mice were weighed prior to surgery and four weeks after before euthanasia. Group 1 being the control (SPION-siScrambled), group 2 SPION-siKRAS, group 3 Gal-1 inh, and group 4 SPION-siKRAS + Gal-1 inh

3.3 Tumor size and weight post dissection

The tumor was measured after extraction. Tumors were also weighed after extraction extrapolating the measurements above.

3.4 SPION-siKRAS + Galectin-1 inhibitor combination treatment reduced tumor weight in -*KRAS^{G12D}; LSL-Trp53^{R172H}* syngeneic mouse model of PDAC

In this chapter we evaluate the efficacy of conjugated SPION-siKRAS + Gal-1 inh. Figure below depicts image (Figure 20 A) and weight (Figure 20 B) of tumor after extraction. Additionally, the orthotopic tumors were visualized at week 0 before treatment and week 5 using animal imaging system (Figure 20 C). Based on these parameters, we observe the weight of the control group being higher when compared to treatment groups. Additionally, the mice treated with combination treatment of SPION-siKRAS and Gal-1 showed decrease in tumor weight as

compared to control (P value 0.001) and siKRAS alone (P<0.01) which by conventional criteria is considered to be statistically significant. Most importantly, out of 4 groups, all the mice from SPION-siKRAS and Gal-1 group survived until the end of the study when all mice from rest of the groups reached endpoint (abdominal diameter of ≥35 mm) or died. Based on these results we can conclude that treatment group SPION-siKRAS + Gal-1 inh showed significant inhibition in tumor growth. We observed that the mice treated with SPION-si-scrambled died the earliest when compared with treatment groups (SPION-siKRAS, Gal-1 inh, and SPION-siKRAS + Gal-1 inh). This signifies that SPION-siKRAS + Gal-1 inh conjugation could have a role in survival.

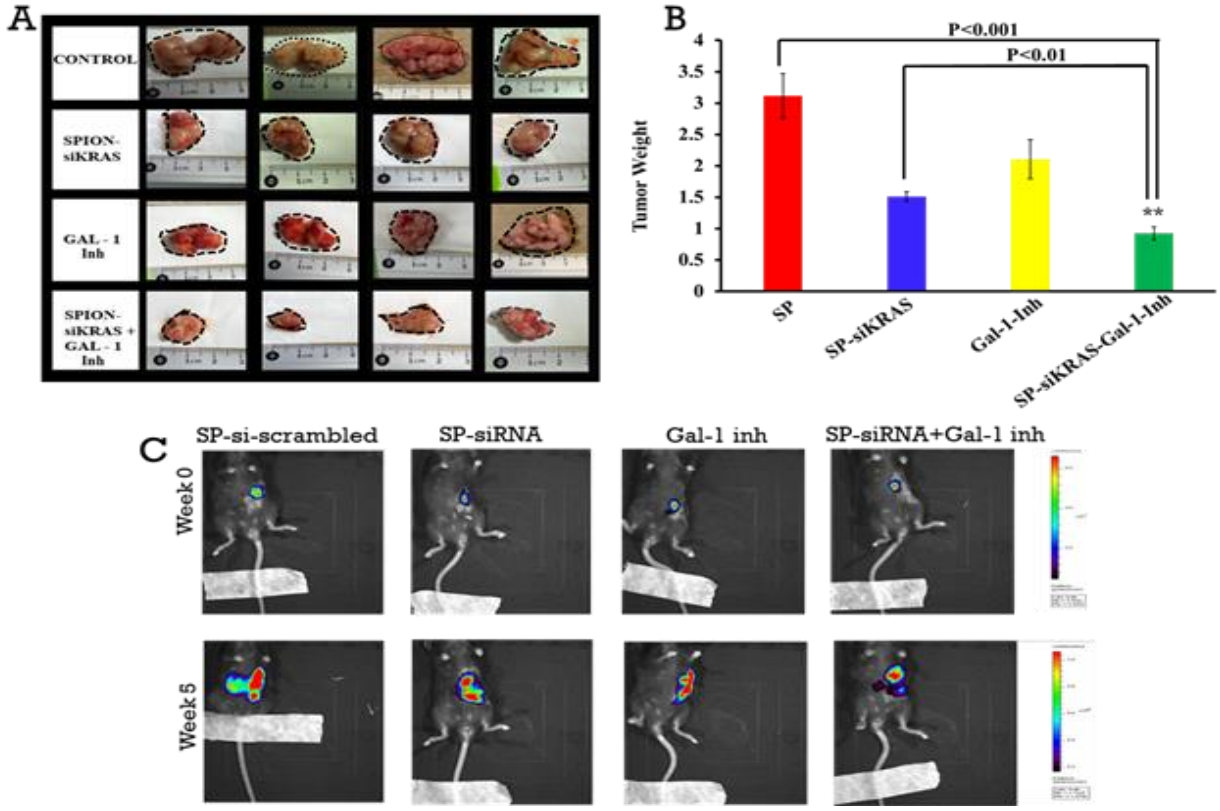

Figure 20. Effect of treatment on tumor burden in mice A) Excised tumors imaged at end point. B) Weight of pancreatic tumor tissue C) Bioluminescence to monitor tumor growth from week 0 to week 5. Luciferase labelled KPC cells (1×10^6) were orthotopically implanted in C5BL6 mice.

3.5 SPION-siKRAS + Galectin-1 inhibitor combination treatment improved survival in - *KRAS^{G12D}; LSL-Trp53^{R172H}* syngeneic mouse model of PDAC

Effects of treatment on pancreatic mice survival and metastasis were analyzed. Excised tumor and organs (liver, lungs, spleen, kidney, heart, and brain) and of all the groups were carefully analyzed. Mice were euthanized five weeks post-surgery unless deceased of natural causation. The control group (SPION-siScrambled) had one survivor when euthanasia was performed. All the animals in the control group (SPION-siScrambled), including the peritoneal cavity and intestines, had a significant rate of metastasis into distant organs, including the lungs and liver (5 mice). Ascites was observed on 4 mice and 3 mice showed signs of splenomegaly. Group two (SPION-siKRAS) had four survivors at time of euthanasia and showed minimal intestinal (1 mice) and liver (1 mice) metastasis. Group three (Gal-1 inh) had three survivors at time of euthanasia, findings include ascites (2 mice), intestinal metastasis (2 mice), and enlarged spleen (1 mice). In Group four (SPION-siKRAS + Gal-1 inh), all members of this group survived till the completion of the study, all five mice were euthanized at this time, observations include no metastasis. From these results we can conclude that treatment group four indicates this novel combination of SPION-siRNA and Gal-1 inh can serve as an excellent potential therapeutic combined treatment.

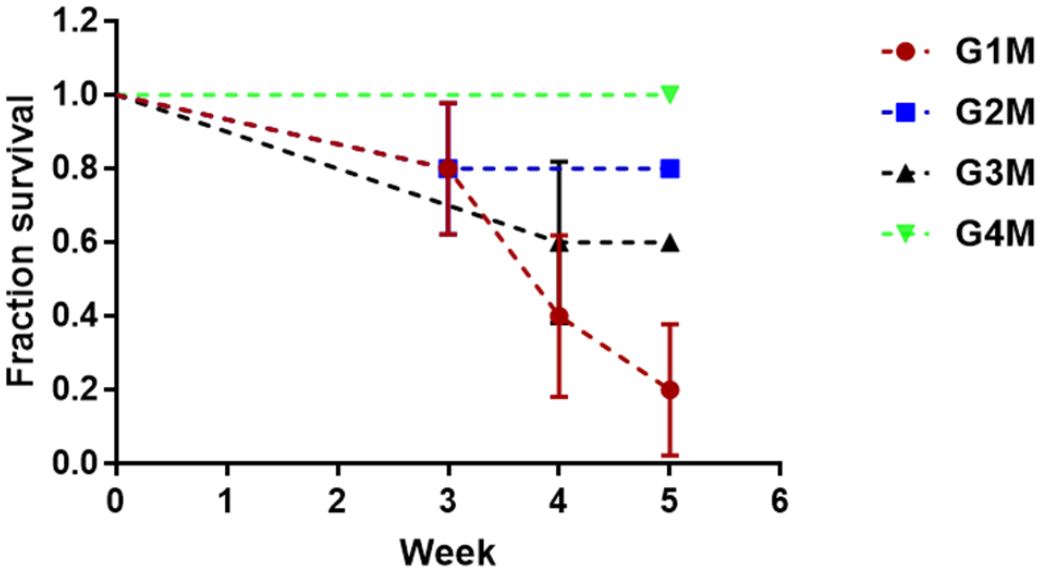

Figure 21. Tumor survival curve Survival curves represent the effect of combined therapy on mice survival.

3.6 Combination therapy reprogrammed myeloid cells, stimulated memory cells, and inhibited regulatory T cells (Tregs) to boost the chemotherapy

The SPION-siRNA in combination with Gal-1 inh showed increased Tcell infiltration and decreased immunosuppressive cells; Treg and M-MDSC. Vehicle-treated group, SPION-siRNA and gal-1 inh alone showed significantly increased levels of myeloid-derived suppressor cells (mMDSCs) i. e CD45+, CD3-, CD11b+, Ly6C high, Ly6G- and T-Regulatory cells (Treg) ie. FoxP3+CD25+CD45+CD3+ cells in *KRAS^{G12D}; LSL-Trp53R172H* syngeneic mouse model of PDAC (Figure 23). Interestingly, the combined treatment reduced the population by approximately 50% and 25%, respectively (Figure 23.). Similar results were observed in memory T cells and CD8+ Tcells, which showed increase in memory T cells (by 1.5 folds) and Tregs (by 2 folds) as compared with SPsiRNA and gal-1 inh alone. These data confirm that effects of SPION-siRNA in combination with Gal-1 inh on immune checkpoint expression on myeloid

cells and thus provide the rationale for combination treatment with SPION-siRNA in combination with Gal-1 inh for immune cell activation. Overall, reduced immune tolerance, increased infiltration of total T cell population and CD8+T cells are observed in mice treated with combination regimen.

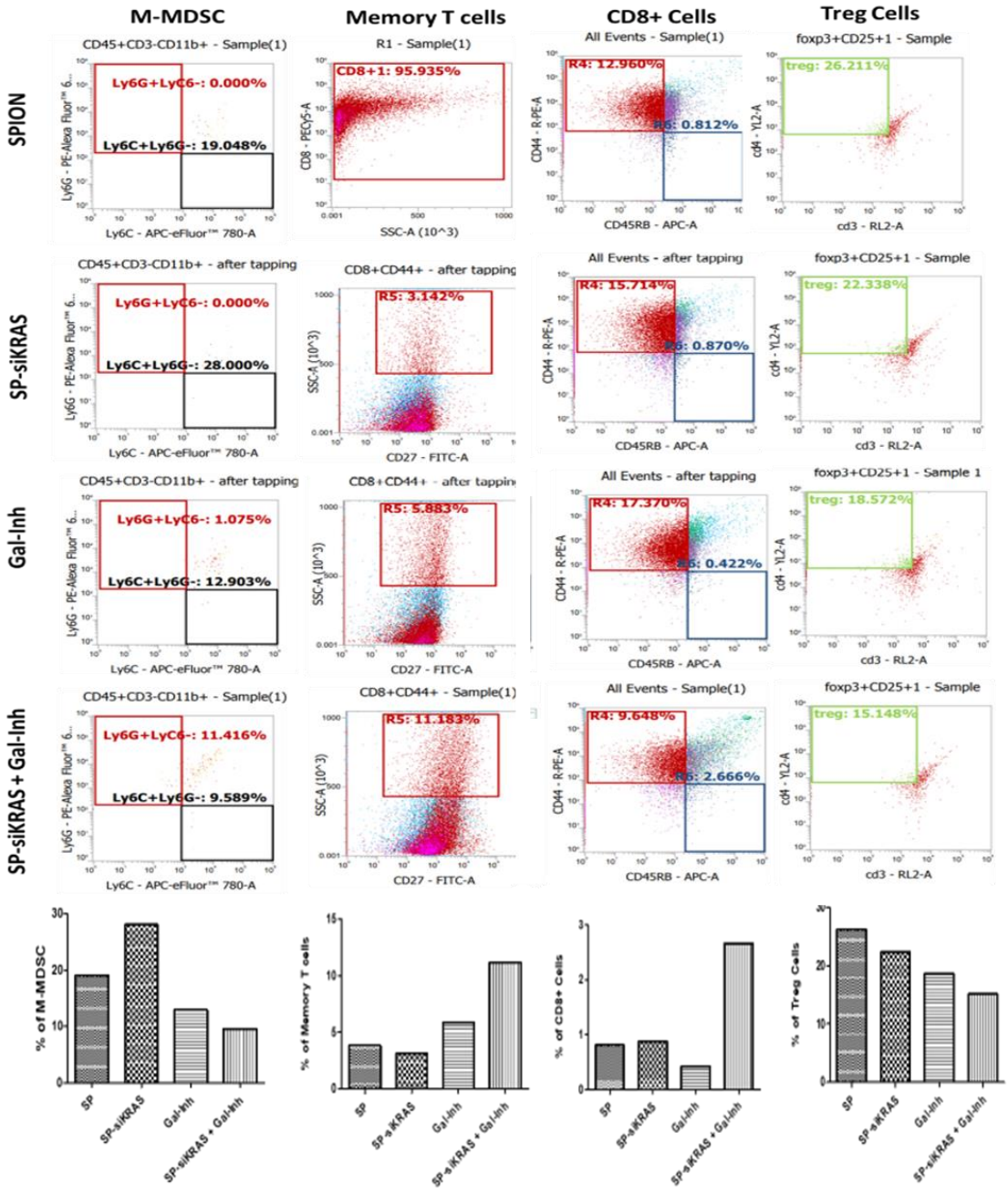

Figure 22 Flow analysis for investigating the immunostimulatory effect of combined therapy of SPION-siKRAS-Gal-inh.

4. Discussion

Increased tumor microenvironmental fibrosis and cancer–stroma crosstalk inside developing tumors restricts medication efficacy due to signaling pathways that impede drug delivery, activation, and effectiveness (Khan *et al*. 2019). The abnormal activation or dysregulation of many signaling pathways contributes significantly to the heterogeneity of pancreatic cancer. The KRAS proto-oncogene encodes for a protein with GTPase activity. $KRAS^{G12D}$ mutation causes constitutive phosphorylation and activation of this pathway (Eser *et al*. 2014). KRAS mutations activate many signaling pathways, including RAF, MEK, ERK, and the P13K/AKT pathway (Knickelbein and Zhang 2015) that play essential roles in cell division, survival, and drug resistance, as well as suppressing apoptosis and increasing tumor development and progression. KRAS activity can alter the microenvironment of PDAC by generating molecules such as Sonic Hedgehog (Ji *et al*. 2007), interleukin-6 (Lesina *et al*. 2011), and prostaglandin E (Charo *et al*. 2013), and hence govern stroma maintenance (Pylayeva-Gupta *et al*. 2012). KRAS signaling has also been demonstrated to promote immunosuppression. SiRNA treatments have been employed in the goal of reducing the progression of pancreatic cancer in order to overcome drug resistance, reduce off-target toxicity, and increase antitumor activity of chemotherapeutic drugs(Aslan *et al*. 2018).

In this study we have propose (chapter III) the therapeutic efficacy of a patented SPION nano-formulation (Yallapu *et al*. 2011) with the conjugation of silencer siRNA-$KRAS^{G12D}$ and the simultaneous delivery of Gal-1 inh (DB21). Our initial objective was to create and characterize the formulation (SPION-siKRAS). The final formulation has a size of 125 nm and a zeta potential of 19 mV, making it an appropriate delivery vehicle for cancer treatment. In a prior study, we employed this SPION formulation to deliver curcumin to PanCa cells *via* miR-145

(Khan *et al*. 2014); this unique formulation was neither harmful to normal nor cancer cells. Secondly, and addition of Gal-1 inh was proposed for this study, for the targeting and suppression of stromal talk and TME. The tumor microenvironment contains a range of cells (stellate cells, pan-endothelial cells, and infiltrating immune cells such as MDSC, Treg cells, and tumor-associated macrophages) and extracellular matrix (ECM) components with blood vessels and neurons.

The in vivo data showed that SPION-siKRAS and the combination of Gal-1 inh improved survival in the C57BL/6 mouse model. Tumor volume was effectively suppressed in those treated with SPION-siKRAS plus a combined Gal-1 inh. Furthermore, as compared to these therapies delivered alone, successfully increased the rate of survival in these treated groups (Figure 21). This was corroborated by tumor size and weight as well as immune profiling using flow cytometry. SPION-siRNA in conjunction with a Gal-1 inh enhanced T-cell infiltration while decreasing immunosuppressive cells such as Treg and M-MDSC. Overall, mice treated with the combined regimen had decreased immunological tolerance and increased infiltration of total T cell population and CD8+T cells.

This promising study depicts in the *in vivo* results that SPION-siKRAS and combination of Gal-1 inh enhanced targeted approach in C57BL/6 mouse model. It has been observed that SPION-siKRAS + Gal-1 inh combinatorial effects improves survival and metastasis expansion rate (Figure 21). Tumor volume was efficiently controlled in SPION-siKRAS + Gal-1 inh. Also, effectively enhanced the rate of survival in these treated groups when compared to control (Figure 21). This was supported with tumor weight and size as well as observation at time of dissection (Figure 20). The combination therapy reduced immune tolerance, increased infiltration

of total T cell population and CD8+T cells are observed in mice treated with combination regimen.

5. Conclusion

In conclusion, results indicate high significance of targeted SPION-siKRAS + Gal-1 inh for achieving targeted pancreatic tumor specific delivery of proposed treatment. Since SPION-siRNA particles inhibit KRAS, KRAS pathway expression, and slowing KRAS-driven pancreatic cancer growth *in vitro* and *in vivo*. Because Gal-1 regulates paracrine interactions with epithelial cells to promote proliferation, migration, tumor transformation, and invasion, as well as endothelial and inflammatory cells to promote angiogenesis and immune cell suppression, inhibiting Gal-1 in conjunction with silencing mutated KRAS has the potential to inhibit tumor growth and progression, as demonstrated in this chapter. This research has the potential to reduce disease-related morbidity and mortality while potentially increasing patient survival.

REFERENCES

Ahmad, Nisar, Hans-J Gabius, Subramanian Sabesan, Stefan Oscarson, and C Fred Brewer. 2004. 'Thermodynamic binding studies of bivalent oligosaccharides to galectin-1, galectin-3, and the carbohydrate recognition domain of galectin-3', *Glycobiology*, 14: 817-25.

Aslan, Minela, Reza Shahbazi, Kezban Ulubayram, and Bulent Ozpolat. 2018. 'Targeted therapies for pancreatic cancer and hurdles ahead', *Anticancer research*, 38: 6591-606.

Astorgues-Xerri, Lucile, Maria E Riveiro, Annemilaï Tijeras-Raballand, Maria Serova, Cindy Neuzillet, Sébastien Albert, Eric Raymond, and Sandrine Faivre. 2014. 'Unraveling galectin-1 as a novel therapeutic target for cancer', *Cancer treatment reviews*, 40: 307-19.

Balkwill, Fran, and Alberto Mantovani. 2001. 'Inflammation and cancer: back to Virchow?', *The Lancet*, 357: 539-45.

Barondes, Samuel H, DNW Cooper, Michael A Gitt, and Hakon Leffler. 1994. 'Galectins. Structure and function of a large family of animal lectins', *The Journal of biological chemistry*, 269: 20807-10.

Bellizzi, Andrew M, Mark Bloomston, Xiao-Ping Zhou, Obiajulu Hans Iwenofu, and Wendy L Frankel. 2010. 'The mTOR pathway is frequently activated in pancreatic ductal adenocarcinoma and chronic pancreatitis', *Applied Immunohistochemistry & Molecular Morphology*, 18: 442-47.

Bergers, Gabriele, and Douglas Hanahan. 2008. 'Modes of resistance to anti-angiogenic therapy', *Nature Reviews Cancer*, 8: 592-603.

Biankin, Andrew V, James G Kench, Sandra A Biankin, C-Soon Lee, Adrienne L Morey, Floriaan P Dijkman, Maxwell J Coleman, Robert L Sutherland, and Susan M Henshall. 2004. 'Pancreatic intraepithelial neoplasia in association with intraductal papillary mucinous neoplasms of the pancreas: implications for disease progression and recurrence', *The American journal of surgical pathology*, 28: 1184-92.

Biankin, Andrew V, Nicola Waddell, Karin S Kassahn, Marie-Claude Gingras, Lakshmi B Muthuswamy, Amber L Johns, David K Miller, Peter J Wilson, Ann-Marie Patch, and Jianmin Wu. 2012. 'Pancreatic cancer genomes reveal aberrations in axon guidance pathway genes', *Nature*, 491: 399-405.

Biffi, G., T. E. Oni, B. Spielman, Y. Hao, E. Elyada, Y. Park, J. Preall, and D. A. Tuveson. 2019. 'IL1-Induced JAK/STAT Signaling Is Antagonized by TGFβ to Shape CAF Heterogeneity in Pancreatic Ductal Adenocarcinoma', *Cancer Discov*, 9: 282-301.

Bramhall, Simon R, John P Neoptolemos, Gordon WH Stamp, and Nicholas R Lemoine. 1997. 'Imbalance of expression of matrix metalloproteinases (MMPs) and tissue inhibitors of the matrix metalloproteinases (TIMPs) in human pancreatic carcinoma', *The Journal of Pathology: A Journal of the Pathological Society of Great Britain and Ireland*, 182: 347-55.

Bryant, Kirsten L, Joseph D Mancias, Alec C Kimmelman, and Channing J Der. 2014. 'KRAS: feeding pancreatic cancer proliferation', *Trends in biochemical sciences*, 39: 91-100.

Caldas, Carlos, and Scott E Kern. 1995. 'K-ras mutation and pancreatic adenocarcinoma', *International journal of pancreatology*, 18: 1-6.

Calhoun, Eric S, Jessa B Jones, Raheela Ashfaq, Volkan Adsay, Suzanne J Baker, Virginia Valentine, Paula M Hempen, Werner Hilgers, Charles J Yeo, and Ralph H Hruban. 2003. 'BRAF and FBXW7 (CDC4, FBW7, AGO, SEL10) mutations in distinct subsets of pancreatic cancer: potential therapeutic targets', *The American journal of pathology*, 163: 1255-60.

Camby, Isabelle, Marie Le Mercier, Florence Lefranc, and Robert Kiss. 2006. 'Galectin-1: a small protein with major functions', *Glycobiology*, 16: 137R-57R.

Chang, Kenneth J, Gulshan Parasher, Catherine Christie, Joan Largent, and Hoda Anton-Culver. 2005. 'Risk of pancreatic adenocarcinoma: disparity between African Americans and other race/ethnic groups', *Cancer*, 103: 349-57.

Chang, Qing, Igor Jurisica, Trevor Do, and David W Hedley. 2011. 'Hypoxia predicts aggressive growth and spontaneous metastasis formation from orthotopically grown primary xenografts of human pancreatic cancer', *Cancer research*, 71: 3110-20.

Charo, Chantale, Vijaykumar Holla, Thiruvengadam Arumugam, Rosa Hwang, Peiying Yang, Raymond N Dubois, David G Menter, Craig D Logsdon, and Vijaya Ramachandran. 2013. 'PGE2 regulates pancreatic stellate cell activity via the EP4 receptor', *Pancreas*, 42: 467.

Chen, X., and E. Song. 2019. 'Turning foes to friends: targeting cancer-associated fibroblasts', *Nat Rev Drug Discov*, 18: 99-115.

Cheng, Jin Quan, Bruce Ruggeri, Walter M Klein, Gonosuke Sonoda, Deborah A Altomare, Dennis K Watson, and Joseph R Testa. 1996. 'Amplification of AKT2 in human pancreatic cells and inhibition of AKT2 expression and tumorigenicity by antisense RNA', *Proceedings of the National Academy of Sciences*, 93: 3636-41.

Christensen, James, Jill Hallin, Vickie Bowcut, Andrew Calinisan, David Briere, Lauren Hargis, Lars Engstrom, Jade Laguer, James Medwid, and Darin Vanderpool. 2022. 'A Non-covalent KRASG12D Allele Specific Inhibitor Demonstrates Potent Inhibition of KRAS-dependent Signaling and Regression of KRASG12D-mutant Tumors'.

Cicenas, Jonas, Kotryna Kvederaviciute, Ingrida Meskinyte, Edita Meskinyte-Kausiliene, Aiste Skeberdyte, and Jonas Cicenas Jr. 2017. 'KRAS, TP53, CDKN2A, SMAD4, BRCA1, and BRCA2 mutations in pancreatic cancer', *Cancers*, 9: 42.

Clerch, Linda B, Philip Whitney, Michael Hass, Keith Brew, Todd Miller, Rudolf Werner, and Donald Massaro. 1988. 'Sequence of a full-length cDNA for rat lung. beta.-galactoside-binding protein: primary and secondary structure of the lectin', *Biochemistry*, 27: 692-99.

Cohen, Romain, Cindy Neuzillet, Annemilaï Tijeras-Raballand, Sandrine Faivre, Armand de Gramont, and Eric Raymond. 2015. 'Targeting cancer cell metabolism in pancreatic adenocarcinoma', *Oncotarget*, 6: 16832.

Cooper, Caroline L, Sandra A O'Toole, and James G Kench. 2013. 'Classification, morphology and molecular pathology of premalignant lesions of the pancreas', *Pathology*, 45: 286-304.

Dan, Nirnoy, Sheema Khan, Saini Setua, Sonam Kumari, Pallabita Chowdhury, Kamalika Samanta, Meena Jaggi, Murali Yallappu, and Subhash Chauhan. 2019. "Nanodelivery platform for targeting mutant-KRAS and improving response to gemcitabine therapy." In.: AACR.

Dey, Prasenjit, Jun Li, Jianhua Zhang, Surendra Chaurasiya, Anders Strom, Huamin Wang, Wen-Ting Liao, Frederick Cavallaro, Parker Denz, and Vincent Bernard. 2020. 'Oncogenic KRAS-driven metabolic reprogramming in pancreatic cancer cells utilizes cytokines from the tumor microenvironment', *Cancer discovery*, 10: 608-25.

Dias Carvalho, Patrícia, Ana Luísa Machado, Flávia Martins, Raquel Seruca, and Sérgia Velho. 2019. 'Targeting the Tumor Microenvironment: An Unexplored Strategy for Mutant KRAS Tumors', *Cancers*, 11: 2010.

Du, Jiali, Jichun Gu, Junyuan Deng, Lei Kong, Yujie Guo, Chen Jin, Yun Bao, Deliang Fu, and Ji Li. 2022. 'The expression and survival significance of sodium glucose transporters in pancreatic cancer', *BMC cancer*, 22: 1-19.

Eloubeidi, Mohamad A, Renee A Desmond, C Mel Wilcox, Reda J Wilson, Pavan Manchikalapati, Mona M Fouad, Isam Eltoum, and Selwyn M Vickers. 2006. 'Prognostic factors for survival in pancreatic cancer: a population-based study', *The American Journal of Surgery*, 192: 322-29.

Elyada, E., M. Bolisetty, P. Laise, W. F. Flynn, E. T. Courtois, R. A. Burkhart, J. A. Teinor, P. Belleau, G. Biffi, M. S. Lucito, S. Sivajothi, T. D. Armstrong, D. D. Engle, K. H. Yu, Y.

Hao, C. L. Wolfgang, Y. Park, J. Preall, E. M. Jaffee, A. Califano, P. Robson, and D. A. Tuveson. 2019. 'Cross-Species Single-Cell Analysis of Pancreatic Ductal Adenocarcinoma Reveals Antigen-Presenting Cancer-Associated Fibroblasts', *Cancer Discov*, 9: 1102-23.

Eser, S, A Schnieke, G Schneider, and D Saur. 2014. 'Oncogenic KRAS signalling in pancreatic cancer', *British Journal of Cancer*, 111: 817-22.

Feig, C., J. O. Jones, M. Kraman, R. J. Wells, A. Deonarine, D. S. Chan, C. M. Connell, E. W. Roberts, Q. Zhao, O. L. Caballero, S. A. Teichmann, T. Janowitz, D. I. Jodrell, D. A. Tuveson, and D. T. Fearon. 2013. 'Targeting CXCL12 from FAP-expressing carcinoma-associated fibroblasts synergizes with anti-PD-L1 immunotherapy in pancreatic cancer', *Proc Natl Acad Sci U S A*, 110: 20212-7.

Feldmann, Georg, and Anirban Maitra. 2008. 'Molecular genetics of pancreatic ductal adenocarcinomas and recent implications for translational efforts', *The Journal of Molecular Diagnostics*, 10: 111-22.

Fischer, Christian, Hugo Sanchez-Ruderisch, Martina Welzel, Bertram Wiedenmann, Toshiyuki Sakai, Sabine André, Hans-Joachim Gabius, Levon Khachigian, Katharina M Detjen, and Stefan Rosewicz. 2005. 'Galectin-1 interacts with the α5β1 fibronectin receptor to restrict carcinoma cell growth via induction of p21 and p27', *Journal of Biological Chemistry*, 280: 37266-77.

Golan, Talia, Elina Zorde Khvalevsky, Ayala Hubert, Rachel Malka Gabai, Naama Hen, Amiel Segal, Abraham Domb, Gil Harari, Eliel Ben David, and Stephen Raskin. 2015. 'RNAi therapy targeting KRAS in combination with chemotherapy for locally advanced pancreatic cancer patients', *Oncotarget*, 6: 24560.

Golay, Hadrien G, and David A Barbie. 2014. "Targeting cytokine networks in KRAS-driven tumorigenesis." In, 869-71. Taylor & Francis.

Golčić, Marin, Luka Simetić, Tea Majnarić, Goran Golčić, and Davorin Herceg. 2022. 'Could fecal microbial transplantation offer a new potential in the treatment of metastatic pancreatic ductal adenocarcinoma?', *Medical Hypotheses*, 161: 110801.

Griffin, Constance A, Ralph H Hruban, Laura A Morsberger, Tara Ellingham, Patricia P Long, Elizabeth M Jaffee, Karen M Hauda, Stefan K Bohlander, and Charles J Yeo. 1995. 'Consistent chromosome abnormalities in adenocarcinoma of the pancreas', *Cancer research*, 55: 2394-99.

Guillaumond, Fabienne, Julie Leca, Orianne Olivares, Marie-Noëlle Lavaut, Nicolas Vidal, Patrice Berthezène, Nelson Javier Dusetti, Céline Loncle, Ezequiel Calvo, and Olivier Turrini. 2013. 'Strengthened glycolysis under hypoxia supports tumor symbiosis and hexosamine biosynthesis in pancreatic adenocarcinoma', *Proceedings of the National Academy of Sciences*, 110: 3919-24.

Guo, Junli, Keping Xie, and Shaojiang Zheng. 2016. 'Molecular biomarkers of pancreatic intraepithelial neoplasia and their implications in early diagnosis and therapeutic intervention of pancreatic cancer', *International journal of biological sciences*, 12: 292.

Hamarsheh, S., O. Groß, T. Brummer, and R. Zeiser. 2020. 'Immune modulatory effects of oncogenic KRAS in cancer', *Nat Commun*, 11: 5439.

Hingorani, Sunil R, Emanuel F Petricoin III, Anirban Maitra, Vinodh Rajapakse, Catrina King, Michael A Jacobetz, Sally Ross, Thomas P Conrads, Timothy D Veenstra, and Ben A Hitt. 2003. 'Preinvasive and invasive ductal pancreatic cancer and its early detection in the mouse', *Cancer cell*, 4: 437-50.

Hingorani, Sunil R, Lifu Wang, Asha S Multani, Chelsea Combs, Therese B Deramaudt, Ralph H Hruban, Anil K Rustgi, Sandy Chang, and David A Tuveson. 2005. 'Trp53R172H and KrasG12D cooperate to promote chromosomal instability and widely metastatic pancreatic ductal adenocarcinoma in mice', *Cancer cell*, 7: 469-83.

Hirt, Christian K, Tijmen H Booij, Linda Grob, Patrik Simmler, Nora C Toussaint, David Keller, Doreen Taube, Vanessa Ludwig, Alexander Goryachkin, and Chantal Pauli. 2022. 'Drug screening and genome editing in human pancreatic cancer organoids identifies drug-gene interactions and candidates for off-label therapy', *Cell genomics*, 2: 100095.

Hong, David S., Marwan G. Fakih, John H. Strickler, Jayesh Desai, Gregory A. Durm, Geoffrey I. Shapiro, Gerald S. Falchook, Timothy J. Price, Adrian Sacher, Crystal S. Denlinger, Yung-Jue Bang, Grace K. Dy, John C. Krauss, Yasutoshi Kuboki, James C. Kuo, Andrew L. Coveler, Keunchil Park, Tae Won Kim, Fabrice Barlesi, Pamela N. Munster, Suresh S. Ramalingam, Timothy F. Burns, Funda Meric-Bernstam, Haby Henary, Jude Ngang, Gataree Ngarmchamnanrith, June Kim, Brett E. Houk, Jude Canon, J. Russell Lipford, Gregory Friberg, Piro Lito, Ramaswamy Govindan, and Bob T. Li. 2020. 'KRAS(G12C) Inhibition with Sotorasib in Advanced Solid Tumors', *The New England journal of medicine*, 383: 1207-17.

Hosein, Abdel Nasser, Stephanie K Dougan, Andrew J Aguirre, and Anirban Maitra. 2022. 'Translational advances in pancreatic ductal adenocarcinoma therapy', *Nature cancer*, 3: 272-86.

Hruban, Ralph H, N Volkan Adsay, Jorge Albores–Saavedra, Carolyn Compton, Elizabeth S Garrett, Steven N Goodman, Scott E Kern, David S Klimstra, Günter Klöppel, and Daniel S Longnecker. 2001. 'Pancreatic intraepithelial neoplasia: a new nomenclature and classification system for pancreatic duct lesions', *The American journal of surgical pathology*, 25: 579-86.

Hughes, R Colin. 1999. 'Secretion of the galectin family of mammalian carbohydrate-binding proteins', *Biochimica et Biophysica Acta (BBA)-General Subjects*, 1473: 172-85.

Izuishi, Kunihiko, Kazuyoshi Kato, Tsutomu Ogura, Taira Kinoshita, and Hiroyasu Esumi. 2000. 'Remarkable tolerance of tumor cells to nutrient deprivation: possible new biochemical target for cancer therapy', *Cancer research*, 60: 6201-07.

Jacobetz, M. A., D. S. Chan, A. Neesse, T. E. Bapiro, N. Cook, K. K. Frese, C. Feig, T. Nakagawa, M. E. Caldwell, H. I. Zecchini, M. P. Lolkema, P. Jiang, A. Kultti, C. B. Thompson, D. C. Maneval, D. I. Jodrell, G. I. Frost, H. M. Shepard, J. N. Skepper, and D. A. Tuveson. 2013. 'Hyaluronan impairs vascular function and drug delivery in a mouse model of pancreatic cancer', *Gut*, 62: 112-20.

Janssen, Quisette P, Stefan Buettner, Mustafa Suker, Berend R Beumer, Pietro Addeo, Philippe Bachellier, Nathan Bahary, Tanios Bekaii-Saab, Maria A Bali, and Marc G Besselink. 2019. 'Neoadjuvant FOLFIRINOX in patients with borderline resectable pancreatic cancer: a systematic review and patient-level meta-analysis', *JNCI: Journal of the National Cancer Institute*, 111: 782-94.

Ji, Zhenyu, Fang C Mei, Jingwu Xie, and Xiaodong Cheng. 2007. 'Oncogenic KRAS activates hedgehog signaling pathway in pancreatic cancer cells', *Journal of Biological Chemistry*, 282: 14048-55.

Jonckheere, Nicolas, Romain Vasseur, and Isabelle Van Seuningen. 2017. 'The cornerstone K-RAS mutation in pancreatic adenocarcinoma: From cell signaling network, target genes, biological processes to therapeutic targeting', *Critical reviews in oncology/hematology*, 111: 7-19.

Jones, Lucie E, Michelle J Humphreys, Fiona Campbell, John P Neoptolemos, and Mark T Boyd. 2004. 'Comprehensive analysis of matrix metalloproteinase and tissue inhibitor expression in pancreatic cancer: increased expression of matrix metalloproteinase-7 predicts poor survival', *Clinical Cancer Research*, 10: 2832-45.

Jones, Siân, Xiaosong Zhang, D Williams Parsons, Jimmy Cheng-Ho Lin, Rebecca J Leary, Philipp Angenendt, Parminder Mankoo, Hannah Carter, Hirohiko Kamiyama, and Antonio Jimeno. 2008. 'Core signaling pathways in human pancreatic cancers revealed by global genomic analyses', *science*, 321: 1801-06.

Jonsson, Jörgen, Lena Carlsson, Thomas Edlund, and Helena Edlund. 1994. 'Insulin-promoter-factor 1 is required for pancreas development in mice', *Nature*, 371: 606-09.

Kamerkar, Sushrut, Valerie S LeBleu, Hikaru Sugimoto, Sujuan Yang, Carolina F Ruivo, Sonia A Melo, J Jack Lee, and Raghu Kalluri. 2017. 'Exosomes facilitate therapeutic targeting of oncogenic KRAS in pancreatic cancer', *Nature*, 546: 498-503.

Kamisawa, Terumi, Laura D Wood, Takao Itoi, and Kyoichi Takaori. 2016. 'Pancreatic cancer', *The Lancet*, 388: 73-85.

Kargozaran, Hamed, Vu Vu, Partha Ray, Sanjay Bagaria, Shawn Steen, Xing Ye, and Singh Gagandeep. 2011. 'Invasive IPMN and MCN: same organ, sifferent outcomes?', *Annals of surgical oncology*, 18: 345-51.

Khan, S., M. C. Ebeling, M. S. Zaman, M. Sikander, M. M. Yallapu, N. Chauhan, A. M. Yacoubian, S. W. Behrman, N. Zafar, D. Kumar, P. A. Thompson, M. Jaggi, and S. C. Chauhan. 2014. 'MicroRNA-145 targets MUC13 and suppresses growth and invasion of pancreatic cancer', *Oncotarget*, 5: 7599-609.

Khan, Sheema, Saini Setua, Sonam Kumari, Nirnoy Dan, Andrew Massey, Bilal Bin Hafeez, Murali M Yallapu, Zachary Edwar Stiles, Anas Alabkaa, and Junming Yue. 2019. 'Superparamagnetic iron oxide nanoparticles of curcumin enhance gemcitabine therapeutic response in pancreatic cancer', *Biomaterials*, 208: 83-97.

Khorana, Alok A, Pamela B Mangu, Jordan Berlin, Anitra Engebretson, Theodore S Hong, Anirban Maitra, Supriya G Mohile, Matthew Mumber, Richard Schulick, and Marc Shapiro. 2016. 'Potentially curable pancreatic cancer: American Society of Clinical Oncology clinical practice guideline', *Journal of Clinical Oncology*, 34: 2541-56.

Kim, Hyun Jin, Ahram Kim, Kanjiro Miyata, and Kazunori Kataoka. 2016. 'Recent progress in development of siRNA delivery vehicles for cancer therapy', *Advanced drug delivery reviews*, 104: 61-77.

Kitajima, Shunsuke, Rohit Thummalapalli, and David A Barbie. 2016. "Inflammation as a driver and vulnerability of KRAS mediated oncogenesis." In *Seminars in cell & developmental biology*, 127-35. Elsevier.

Knickelbein, Kyle, and Lin Zhang. 2015. 'Mutant KRAS as a critical determinant of the therapeutic response of colorectal cancer', *Genes & diseases*, 2: 4-12.

Kokkinos, J., R. M. C. Ignacio, G. Sharbeen, C. Boyer, E. Gonzales-Aloy, D. Goldstein, Apgi Australian Pancreatic Cancer Genome Initiative, J. A. McCarroll, and P. A. Phillips. 2020. 'Targeting the undruggable in pancreatic cancer using nano-based gene silencing drugs', *Biomaterials*, 240: 119742.

Koorstra, Jan-Bart M, Georg Feldmann, Nils Habbe, and Anirban Maitra. 2008. 'Morphogenesis of pancreatic cancer: role of pancreatic intraepithelial neoplasia (PanINs)', *Langenbeck's archives of surgery*, 393: 561-70.

Lee, Jae W, Chad A Komar, Fee Bengsch, Kathleen Graham, and Gregory L Beatty. 2016. 'Genetically engineered mouse models of pancreatic cancer: the KPC model (LSL-KrasG12D/+; LSL-Trp53R172H/+; Pdx-1-Cre), its variants, and their application in immuno-oncology drug discovery', *Current protocols in pharmacology*, 73: 14.39. 1-14.39. 20.

Lesina, Marina, Magdalena U Kurkowski, Katharina Ludes, Stefan Rose-John, Matthias Treiber, Günter Klöppel, Akihiko Yoshimura, Wolfgang Reindl, Bence Sipos, and Shizuo Akira.

2011. 'Stat3/Socs3 activation by IL-6 transsignaling promotes progression of pancreatic intraepithelial neoplasia and development of pancreatic cancer', *Cancer cell*, 19: 456-69.

Löhr, Matthias, Gunter Klöppel, Patrick Maisonneuve, Albert B Lowenfels, and Jutta Lüttges. 2005. 'Frequency of K-ras mutations in pancreatic intraductal neoplasias associated with pancreatic ductal adenocarcinoma and chronic pancreatitis: a meta-analysis', *Neoplasia*, 7: 17-23.

Luo, Ji. 2021. "KRAS mutation in pancreatic cancer." In *Seminars in oncology*, 10-18. Elsevier.

Maitra, Anirban, and Ralph H Hruban. 2008. 'Pancreatic cancer', *Annu. Rev. Pathol. Mech. Dis.*, 3: 157-88.

Majumder, Kaustav, Nivedita Arora, Shrey Modi, Rohit Chugh, Alice Nomura, Bhuwan Giri, Rajinder Dawra, Sundaram Ramakrishnan, Sulagna Banerjee, and Ashok Saluja. 2016. 'A novel immunocompetent mouse model of pancreatic cancer with robust stroma: a valuable tool for preclinical evaluation of new therapies', *Journal of gastrointestinal surgery*, 20: 53-65.

Manero-Rupérez, Noemí, Neus Martínez-Bosch, Luis E. Barranco, Laura Visa, and Pilar Navarro. 2020. 'The Galectin Family as Molecular Targets: Hopes for Defeating Pancreatic Cancer', *Cells*, 9: 689.

Matsuyama, Yoshito, Sonshin Takao, and Takashi Aikou. 2002. 'Comparison of matrix metalloproteinase expression between primary tumors with or without liver metastasis in pancreatic and colorectal carcinomas', *Journal of surgical oncology*, 80: 105-10.

Mizrahi, Jonathan D, Rishi Surana, Juan W Valle, and Rachna T Shroff. 2020. 'Pancreatic cancer', *The Lancet*, 395: 2008-20.

Okada, Yuji, Guido Eibl, Sushovan Guha, John P Duffy, Howard A Reber, and Oscar J Hines. 2004. 'Nerve growth factor stimulates MMP-2 expression and activity and increases invasion by human pancreatic cancer cells', *Clinical & experimental metastasis*, 21: 285-92.

Organization, World Health. 2012. 'International Agency for Research on Cancer GLOBOCAN 2012: estimated cancer incidence, mortality and prevalence worldwide in 2012', *Lung Cancer*.

Orozco, Carlos A, Neus Martinez-Bosch, Pedro E Guerrero, Judith Vinaixa, Tomás Dalotto-Moreno, Mar Iglesias, Mireia Moreno, Magdolna Djurec, Françoise Poirier, and Hans-Joachim Gabius. 2018. 'Targeting galectin-1 inhibits pancreatic cancer progression by modulating tumor–stroma crosstalk', *Proceedings of the National Academy of Sciences*, 115: E3769-E78.

Ottenhof, Niki A, Roeland F de Wilde, Anirban Maitra, Ralph H Hruban, and G Johan A Offerhaus. 2011. 'Molecular characteristics of pancreatic ductal adenocarcinoma', *Pathology research international*, 2011.

Papke, Bjoern, and Channing J Der. 2017. 'Drugging RAS: Know the enemy', *science*, 355: 1158-63.

Paz, Ariella, Roni Haklai, Galit Elad-Sfadia, Eyal Ballan, and Yoel Kloog. 2001. 'Galectin-1 binds oncogenic H-Ras to mediate Ras membrane anchorage and cell transformation', *Oncogene*, 20: 7486-93.

Pereira, F, A Ferreira, CA Reis, MJ Sousa, MJ Oliveira, and A Preto. 2022. "KRAS as a Modulator of the Inflammatory Tumor Microenvironment: Therapeutic Implications. Cells 2022, 11, 398." In.: s Note: MDPI stays neutral with regard to jurisdictional claims in published ….

Pérez–Mancera, Pedro A, Carmen Guerra, Mariano Barbacid, and David A Tuveson. 2012. 'What we have learned about pancreatic cancer from mouse models', *Gastroenterology*, 142: 1079-92.

Prior, Ian A, Paul D Lewis, and Carla Mattos. 2012. 'A comprehensive survey of Ras mutations in cancer', *Cancer research*, 72: 2457-67.

Pylayeva-Gupta, Yuliya, Kyoung Eun Lee, Cristina H Hajdu, George Miller, and Dafna Bar-Sagi. 2012. 'Oncogenic Kras-induced GM-CSF production promotes the development of pancreatic neoplasia', *Cancer cell*, 21: 836-47.

Rachagani, Satyanarayana, S Senapati, S Chakraborty, Moorthy P Ponnusamy, Sushil Kumar, Lynette M Smith, Maneesh Jain, and Surinder K Batra. 2011. 'Activated KrasG12D is associated with invasion and metastasis of pancreatic cancer cells through inhibition of E-cadherin', *British Journal of Cancer*, 104: 1038-48.

Racu, Marie-Lucie, Laetitia Lebrun, Andrea Alex Schiavo, Claude Van Campenhout, Sarah De Clercq, Lara Absil, Esmeralda Minguijon Perez, Calliope Maris, Christine Decaestecker, and Isabelle Salmon. 2022. 'The Role of SMAD4 Inactivation in Epithelial–Mesenchymal Plasticity of Pancreatic Ductal Adenocarcinoma: The Missing Link?', *Cancers*, 14: 973.

Rawla, Prashanth, Tagore Sunkara, and Vinaya Gaduputi. 2019. 'Epidemiology of pancreatic cancer: global trends, etiology and risk factors', *World journal of oncology*, 10: 10.

Ruggeri, Bruce A, Lingyi Huang, Moira Wood, Jin Quan Cheng, and Joseph R Testa. 1998. 'Amplification and overexpression of the AKT2 oncogene in a subset of human pancreatic ductal adenocarcinomas', *Molecular Carcinogenesis: Published in cooperation with the University of Texas MD Anderson Cancer Center*, 21: 81-86.

Sanchez-Ruderisch, Hugo, Katharina M Detjen, Martina Welzel, Sabine André, Christian Fischer, Hans-Joachim Gabius, and Stefan Rosewicz. 2011. 'Galectin-1 sensitizes carcinoma cells to anoikis via the fibronectin receptor α5β1-integrin', *Cell Death & Differentiation*, 18: 806-16.

Satelli, Arun, Prema S Rao, Prem K Gupta, Paul R Lockman, Kalkunte S Srivenugopal, and U Subrahmanyeswara Rao. 2008. 'Varied expression and localization of multiple galectins in different cancer cell lines', *Oncology reports*, 19: 587-94.

Saxena, Sugandha, Caitlin Molczyk, Abhilasha Purohit, Evie Ehrhorn, Paran Goel, Dipakkumar R Prajapati, Pranita Atri, Sukhwinder Kaur, Paul M Grandgenett, and Michael A Hollingsworth. 2022. 'Differential expression profile of CXC-receptor-2 ligands as potential biomarkers in pancreatic ductal adenocarcinoma', *American journal of cancer research*, 12: 68.

Schlieman, MG, BN Fahy, R Ramsamooj, L Beckett, and Richard J Bold. 2003. 'Incidence, mechanism and prognostic value of activated AKT in pancreas cancer', *British Journal of Cancer*, 89: 2110-15.

Schneiderhan, Wilhelm, Fredy Diaz, Martin Fundel, Shaoxia Zhou, Marco Siech, Cornelia Hasel, Peter Möller, Jürgen E Gschwend, Thomas Seufferlein, and Thomas Gress. 2007. 'Pancreatic stellate cells are an important source of MMP-2 in human pancreatic cancer and accelerate tumor progression in a murine xenograft model and CAM assay', *Journal of cell science*, 120: 512-19.

SEER. "Cancer Stat Facts: Pancreatic Cancer." In. National Cancer Institute ssurveillance eidemiology and end results program: National Cancer Institute

———. 2021. "Cancer Stat Facts: Pancreatic Cancer,." In. https://seer.cancer.gov/statfacts/html/pancreas.html#:~:text=Pancreatic%20cancer%20is: National Cancer Institute (NIH)".

Setten, Ryan L, John J Rossi, and Si-ping Han. 2019. 'The current state and future directions of RNAi-based therapeutics', *Nature Reviews Drug Discovery*, 18: 421-46.

Siegel, Rebecca L, Kimberly D Miller, and Ahmedin Jemal. 2015. 'Cancer statistics, 2015', *CA: a cancer journal for clinicians*, 65: 5-29.

Silverman, Debra T, Robert N Hoover, Linda M Brown, G Marie Swanson, Mark Schiffman, Raymond S Greenberg, Richard B Hayes, Keith D Lillemoe, Janet B Schoenberg, and Ann G Schwartz. 2003. 'Why do Black Americans have a higher risk of pancreatic cancer than White Americans?', *Epidemiology*: 45-54.

Sirivatanauksorn, Vorapan, Yongyut Sirivatanauksorn, Patricia A Gorman, Joanne M Davidson, Denise Sheer, Patrick S Moore, Aldo Scarpa, Paul AW Edwards, and Nicholas R Lemoine. 2001. 'Non-random chromosomal rearrangements in pancreatic cancer cell lines identified by spectral karyotyping', *International journal of cancer*, 91: 350-58.

Society, American Cancer. 2013. "Cancer facts & figures." In.: American Cancer Society, Atlanta.

Tempero, Margaret A, J Pablo Arnoletti, Stephen Behrman, Edgar Ben-Josef, Al B Benson, Jordan D Berlin, John L Cameron, Ephraim S Casper, Steven J Cohen, and Michelle Duff. 2010. 'Pancreatic adenocarcinoma', *Journal of the National Comprehensive Cancer Network*, 8: 972-1017.

Tsai, Yao-Tsung, Chih-Yi Li, Yen-Hua Huang, Te-Sheng Chang, Chung-Yen Lin, Chia-Hsien Chuang, Chih-Yang Wang, Gangga Anuraga, Tzu-Hao Chang, and Tsung-Chieh Shih. 2022. 'Galectin-1 orchestrates an inflammatory tumor-stroma crosstalk in hepatoma by enhancing TNFR1 protein stability and signaling in carcinoma-associated fibroblasts', *Oncogene*: 1-13.

Waddell, Nicola, Marina Pajic, Ann-Marie Patch, David K Chang, Karin S Kassahn, Peter Bailey, Amber L Johns, David Miller, Katia Nones, and Kelly Quek. 2015. 'Whole genomes redefine the mutational landscape of pancreatic cancer', *Nature*, 518: 495-501.

Wang, Shun, Yan Zheng, Feng Yang, Le Zhu, Xiao-Qiang Zhu, Zhe-Fang Wang, Xiao-Lin Wu, Cheng-Hui Zhou, Jia-Yan Yan, and Bei-Yuan Hu. 2021. 'The molecular biology of pancreatic adenocarcinoma: Translational challenges and clinical perspectives', *Signal Transduction and Targeted Therapy*, 6: 1-23.

Wang, Weibin, Carolin Reiser-Erkan, Christoph W Michalski, Matthias C Raggi, Liao Quan, Zhao Yupei, Helmut Friess, Mert Erkan, and Jörg Kleeff. 2010. 'Hypoxia inducible BHLHB2 is a novel and independent prognostic marker in pancreatic ductal adenocarcinoma', *Biochemical and biophysical research communications*, 401: 422-28.

Westphalen, C Benedikt, and Kenneth P Olive. 2012. 'Genetically engineered mouse models of pancreatic cancer', *Cancer journal (Sudbury, Mass.)*, 18: 502.

Wu, Chu, Ping Yang, Bingxue Liu, and Yunlian Tang. 2020. 'Is there a CDKN2A-centric network in pancreatic ductal adenocarcinoma?', *OncoTargets and therapy*, 13: 2551.

Xin, Yong, Min Huang, Wen Wen Guo, Qian Huang, and Guan Jiang. 2017. 'Nano-based delivery of RNAi in cancer therapy', *Molecular cancer*, 16: 1-9.

Yachida, Shinichi, Siân Jones, Ivana Bozic, Tibor Antal, Rebecca Leary, Baojin Fu, Mihoko Kamiyama, Ralph H Hruban, James R Eshleman, and Martin A Nowak. 2010. 'Distant metastasis occurs late during the genetic evolution of pancreatic cancer', *Nature*, 467: 1114-17.

Yallapu, Murali M, Neeraj Chauhan, Shadi F Othman, Vahid Khalilzad-Sharghi, Mara C Ebeling, Sheema Khan, Meena Jaggi, and Subhash C Chauhan. 2015. 'Implications of protein corona on physico-chemical and biological properties of magnetic nanoparticles', *Biomaterials*, 46: 1-12.

Yallapu, Murali M, Mara C Ebeling, Sheema Khan, Vasudha Sundram, Neeraj Chauhan, Brij K Gupta, Susan E Puumala, Meena Jaggi, and Subhash C Chauhan. 2013. 'Novel curcumin-loaded magnetic nanoparticles for pancreatic cancer treatment', *Molecular cancer therapeutics*, 12: 1471-80.

Yallapu, Murali M, Shadi F Othman, Evan T Curtis, Brij K Gupta, Meena Jaggi, and Subhash C Chauhan. 2011. 'Multi-functional magnetic nanoparticles for magnetic resonance imaging and cancer therapy', *Biomaterials*, 32: 1890-905.

Yallapu, Murali Mohan, Brij K Gupta, Meena Jaggi, and Subhash C Chauhan. 2010. 'Fabrication of curcumin encapsulated PLGA nanoparticles for improved therapeutic effects in metastatic cancer cells', *Journal of colloid and interface science*, 351: 19-29.

Yang, Ri-Yao, Gabriel A Rabinovich, and Fu-Tong Liu. 2008. 'Galectins: structure, function and therapeutic potential', *Expert reviews in molecular medicine*, 10.

Zeitouni, Daniel, Yuliya Pylayeva-Gupta, Channing J Der, and Kirsten L Bryant. 2016. 'KRAS mutant pancreatic cancer: no lone path to an effective treatment', *Cancers*, 8: 45.

BIOGRAPHICAL SKETCH

Ana Izavelle Martinez Bulnes is a Honduran native. She graduated from the University of Texas Rio Grande Valley at Texas, United States in 2020 with a Bachelor of Science. She Completed her degree without any experience as an independent researcher. During her bachelor's degree she met Doctor Persans, Professor of Molecular Biology, who encouraged her to continue her studies and fulfil her ultimate potential. His belief continued to carry on to her future. He guided her throughout the application and acceptance into the master's Program. He was the director at the time of the Biochemistry and Molecular Biology Program.

She completed her Master of Science degree in Biochemistry and Molecular Biology in July 2022. She started the discipline of cancer research when she joined the lab at the Biomedical Research Facility, School of Medicine. The research was done under the supervision of Dr. Sheema Khan, Department of Immunology and Microbiology, School of Medicine, University of Texas Rio Grande Valley. She developed a novel strategy to target Pancreatic Ductal Adenocarcinoma with focus on KRAS mutations. She has awarded with Biochemistry and Molecular Biology Master's program Scholarship (BCMB MS) until the completion of her master's, at the University of Texas Rio Grande Valley, Edinburg, Texas. She can be reached at her personal email address ana1997imb@gmail.com